REMARKS

Claims 12, 13, and 37-40 are currently pending in the application. By this amendment, claims 12, 13, 37 and 38 are amended, claims 1, 16-17 and 33-36 are cancelled and new claims 39-40 are added for the Examiner's consideration. The foregoing separate sheets marked as "Listing of Claims" shows all the claims in the application, with an indication of the current status of each.

Applicant thanks Examiner for the courtesy and helpfulness extended during the telephone interview of March 4, 2009. Certain of the present amendments are undertaken in response to Examiner's comments during the interview, namely: 1) removal of the reference to binding site in claim 13; 2) removal of reference to laminin displacement in claims 12 and 13; and 3) change from "judging" to "concluding" in claims 12 and 14. It is Applicant's understanding that, together with the other amendments made in response to rejections in the Office Action of December 23, 2009, these amendments address all issues currently outstanding with respect to the allowance of claims 12, 13 and 37-40.

Claim Rejections: 35 USC § 112, first paragraph

Claims 1,12-13, 16-17 and 33-38 stand rejected under 35 USC § 112, first paragraph, due to a purported lack of enablement. This rejection is traversed.

Claims 1, 35 and 36 have hereby been cancelled, thereby making moot this portion of the rejection.

Applicant thanks Examiner for the clear indication of the subject matter which, according to Examiner, is enabled by the specification as filed, as provided in the last paragraph of page 3 of the Office Action. Claim 12 has hereby been amended accordingly, with the exception that Applicant strongly disagrees with Examiner with respect to limiting the claims to the recitation of an in vivo cell inhibiting effect on melanoma or an in vitro cell inhibiting effect on lung cancer cells in culture.

As discussed in the telephone interview, Applicant herewith provides Examiner additional information and data showing expression of the 67 kDa laminin receptor on the cell surface of a variety of cancer cell types, and the ability of epigallocatechin gallate to bind to the 67 kDa laminin receptor and to cause a decrease in proliferation of cancer cells. In addition, Applicant herewith submits a declaration of the inventor, Dr. Tachibana, which includes data

obtained in his laboratory and under his supervision showing that the action of EGCG in liver cancer cells and breast cancer cells is mediated by the 67 kDa laminin receptor.

The following Table lists the various sources of support for practicing the methods of the invention with respect to lung and melanoma cancer (already agreed to by Examiner) and, in addition, liver cancer, breast cancer, cervical adenocarcinoma cells, multiple myeloma, and colon cancer. Copies of the new sources of support are included herewith as Exhibits A-E.

TYPES OF CANCER CELLS	SUPPORT
lung cancer cells *in vitro*	the present application
melanoma cancer cells *in vivo*	Umeda, J. Biol Chem, 283, 3050-3058 (2008); submitted with previous response
INCLUDED IN THIS COMMUNICATION	
liver cancer cells *in vitro*	**DECLARATION** and data in Figure 1; and **EXHIBIT A**, article in Proceeding of 2004 International Conference O-CHA (tea) culture and Science, 477-478 (2005)
breast cancer cells *in vitro*	**DECLARATION** see data in Figure 2; and **EXHIBIT B** *Nature Struct. Mol. Biol.* 11, 380-381; see Figure 1a, which shows testing of MCF-7 breast cancer cells *in vitro*
cervical cancer cells *in vitro*	**EXHIBIT C** *BBRC*, 333, 337-344 (2005); note Figure 6 in particular
multiple myeloma cells *in vivo* and *in vitro*	**EXHIBIT D** *Blood* 15 October 2008, vol. 108, #8; in this paper, 67LR is referred to as "LR1"; note in particular the data presented in Figure 3
colon cancer cells *in vitro*	**EXHIBIT E** *BBRC* 371 (2008):172-176; note in particular Figures 1 and 4

As can be seen from a review of the information provided herewith, one of skill in the art would recognize that the methods of the invention are applicable to cancer cells in general, as recited in independent claims 12 and 13.

In view of the foregoing, Applicant respectfully requests reconsideration of claims 12 and 13 in their present form and withdrawal of this rejection.

Claim Rejections: 35 USC § 102(b)

Claim 1 stands rejected under 35 USC § 102(b) as anticipated by Narumi et al. (hereinafter "Narumi"). Claim 1 is hereby cancelled without prejudice or disclaimer, thereby making moot this portion of the rejection.

In view of the foregoing, Applicant respectfully requests withdrawal of this rejection.

Claim Rejections: 35 USC § 112, first paragraph, New Matter Rejection

Claims 37 and 38 stand rejected under 35 USC § 112, first paragraph. The Examiner states that there is no support in the specification for an antibody with a galloyl group.

Claims 37 and 38, which depend from claims 12 and 13, respectively, have hereby been amended to clarify the subject matter of the two claims. Claims 37 and 38 now recite that the subject matter of the claims is a method of screening an antibody, i.e. the "compound" referred to in these two claims is the compound that is screened. Applicant submits that this amendment does not add any new matter, being a choice of one of the two possibilities recited in claims 12 and 13, from which claims 37 and 38 depend ("A method of screening a catechin or *antibody*...").

In view of the foregoing, Applicant respectfully requests reconsideration and withdrawal of this rejection.

Claim Rejections: 35 USC § 112, second paragraph

Claim 1, 12-13, 16-17 and 33-38 stand rejected under 35 USC § 112, second paragraph, as indefinite due to the recitation of the relative term "may". Claims 1 and 35-36 are hereby cancelled, making moot this portion of the rejection.

Claims 12 and 13 have hereby been amended to recite" to determine whether" and "has" instead of "may have", thereby overcoming this rejection.

In view of the foregoing, Applicant respectfully requests reconsideration and withdrawal of this rejection.

Claim Rejections: 35 USC § 102(b)

Claim 35 stands rejected under 35 USC § 102(b) as anticipated by Narumi et al. (hereinafter "Narumi"). Claim 35 is hereby cancelled without prejudice or disclaimer, thereby making moot this rejection.

In view of the foregoing, Applicant respectfully requests withdrawal of this rejection.

Concluding Remarks

In view of the foregoing, it is requested that the application be reconsidered, that claims 12, 13, and 37-40 be allowed, and that the application be passed to issue.

Should the Examiner find the application to be other than in condition for allowance, the Examiner is requested to contact the undersigned at 703-787-9400 (fax: 703-787-7557; email: ruth@wcc-ip.com) to discuss any other changes deemed necessary in a telephonic or personal interview.

If an extension of time is required for this response to be considered as being timely filed, a conditional petition is hereby made for such extension of time. Please charge any deficiencies in fees and credit any overpayment of fees to Attorney's Deposit Account No. 50-2041.

Respectfully submitted,

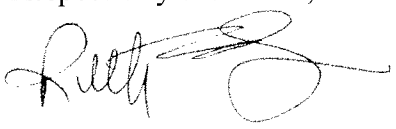

Ruth E. Tyler-Cross
Reg. No. 45,922

Whitham, Curtis, Christofferson & Cook, P.C.
11491 Sunset Hills Road, Suite 340
Reston, VA 20190
703-787-9400 (Telephone)
703-787-7557 (Facsimile)

Exhibit B

A receptor for green tea polyphenol EGCG

Hirofumi Tachibana, Kiyoshi Koga, Yoshinori Fujimura & Koji Yamada

The major polyphenol in green tea, (–)-epigallocatechin-3-gallate (EGCG), has been shown to prevent carcinogenesis. We have identified a receptor that mediates the anticancer activity of EGCG. Expression of the metastasis-associated 67-kDa laminin receptor confers EGCG responsiveness to cancer cells at physiologically relevant concentrations. Experiments using surface plasmon resonance demonstrate binding of EGCG to the 67-kDa laminin receptor with a nanomolar K_d value.

The prevention of cancer through dietary intervention is currently receiving considerable attention. Several epidemiological and animal studies suggest that green tea has a protective effect against a variety of cancer types, such as lung, prostate and breast[1]. This effect has been attributed to the biologically active polyphenol EGCG[2,3]. EGCG has both antimatrix metalloproteinase and antiangiogenesis activities[4,5] that can prevent the formation of solid tumors. The concentration of EGCG (0.1–1 μM) needed to elicit both responses is similar to levels in humans after drinking tea (usually <1 μM; ref. 6). EGCG has also been reported to inhibit cancer cell proliferation directly by affecting the signaling pathways involved in cell growth[7,8]. However, the concentrations of EGCG shown to have an effect (20–100 μM) in these previous studies are much higher than those observed in the blood or tissues. Also, the primary target for EGCG to act upon to elicit cell growth inhibition remains to be determined.

We found that all-*trans*-retinoic acid (ATRA) enhances the binding of EGCG to the cell surface of cancer cells (**Fig. 1a**) when the binding was monitored on the basis of the increase in response units in a surface plasmon resonance assay. To identify candidates through which EGCG inhibits cell growth, we used a subtraction cloning strategy involving cDNA libraries constructed from cells treated or untreated with ATRA. We isolated a single target that allows EGCG to bind to the cell surface. An analysis of the DNA sequence identified this unknown cell surface candidate as the 67-kDa laminin receptor (67 LR). In fact, the expression of this 67 LR was enhanced by ATRA treatment (**Fig. 1a**, inset). The 67 LR is expressed on a variety of tumor cells, and the expression level of this protein strongly correlates with the risk of tumor invasion and metastasis[9,10].

Human lung cancer A549 cells were used to assess how effectively the 67 LR elicits EGCG-mediated growth inhibition. Cells transfected with empty vector and treated with EGCG showed no growth inhibition (**Fig. 1b**, inset, gray bar). However, cells transfected with the

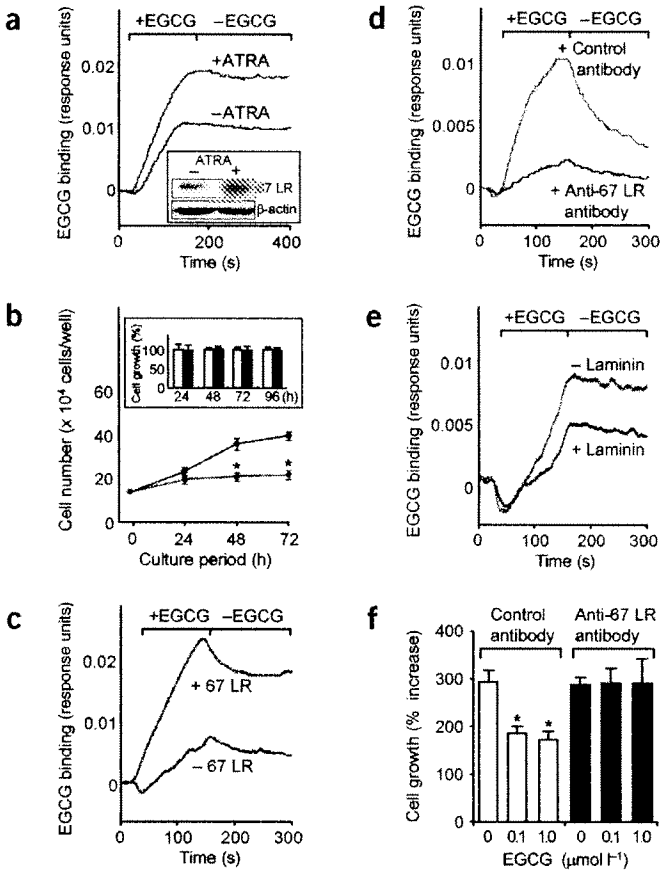

Figure 1 Anticancer action of EGCG is mediated by the 67-kDa laminin receptor. (**a**) EGCG binding to the surface of MCF-7 cells treated with (red line) or without (blue line) ATRA monitored by surface plasmon resonance. Inset, 67 LR and β-actin protein levels from the ATRA-treated or nontreated cells. (**b**) A549 cells transfected with the 67 LR vector were exposed to 5.0 μM EGCG (red line) or water (blue line) for various periods, and the cell numbers were assessed. The cells transfected with the empty vector (inset) were also treated with 5.0 μM EGCG (gray bar) or water (control, white bar), and the results are shown as relative cell number to control cultures at each period. The data presented are the mean (± s.e.m.) of triplicate experiments (asterisk indicates $P < 0.01$). (**c**) The interaction between EGCG (5.0 μM) and A549 cells transfected with the 67 LR vector (red line) or the empty vector (blue line) measured by surface plasmon resonance. (**d**) EGCG binding (1.0 μM) to the 67 LR–transfected cells treated with either anti–67 LR (green line) or control antibody (orange line). (**e**) The interaction between EGCG and 67 LR protein after treatment with either laminin (green line) or BSA (orange line). (**f**) 67 LR–transfected cells treated with either anti–67 LR (gray) or control antibody (white) were cultured in the presence of EGCG. The data presented are the mean (± s.e.m.) of triplicate experiments (asterisk indicates $P < 0.01$).

Department of Bioscience and Biotechnology, Faculty of Agriculture, Kyushu University, Hakozaki 6-10-1, Fukuoka, 812-8581, Japan. Correspondence should be addressed to H.T. (tatibana@agr.kyushu-u.ac.jp).

Published online 14 March 2004; doi:10.1038/nsmb743

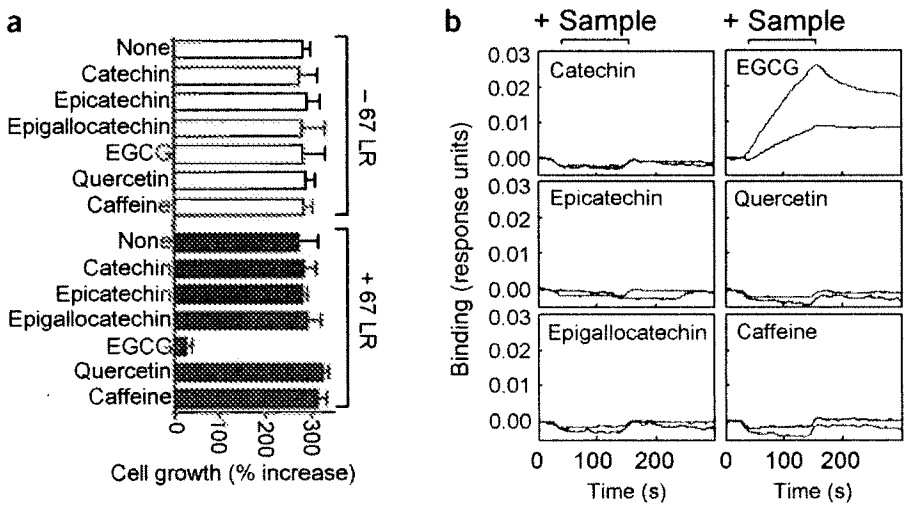

Figure 2 The interactions between tea constituents and 67 LR–transfected cells. (**a**) Growth inhibitory activities of tea constituents (indicated by bars, 5.0 μM) on cells transfected with either the gene encoding 67 LR (gray) or vector only (white) were examined and shown as indicated in **Figure 1f**. (**b**) The interaction between tea constituents (5.0 μM) and A549 cells transfected with the 67 LR vector (red line) or the empty vector (blue line) was measured using a surface plasmon resonance assay.

gene encoding 67 LR and treated with EGCG (**Fig. 1b**, red line) demonstrated considerable inhibition as compared with the cells treated with H_2O (**Fig. 1b**, blue line).

We next tested whether the growth inhibitory activity of EGCG correlates with the binding strength of EGCG to the cell surface. We found increased binding of EGCG to the cell surface of cells transfected with 67 LR (**Fig. 1c**). The number of response units did not return to the basal level after termination of EGCG exposure (**Fig. 1**, –EGCG), indicating that EGCG remains bound even in the absence of EGCG. EGCG binding to the 67 LR–transfected cells was inhibited by treatment with an antibody to 67 LR (**Fig. 1d**). We also tested whether laminin, a known ligand for the 67 LR, can compete with EGCG for binding. Laminin reduced the interaction between EGCG and the 67 LR protein (**Fig. 1e**).

We then measured the binding affinity of EGCG to 67 LR in equilibrium binding experiments using surface plasmon resonance (see **Supplementary Methods** online). K_d measurements were made with a purified recombinant 67 LR protein. The predicted K_d value for the binding of EGCG to the 67 LR protein is 39.9 nM.

To investigate whether the 67 LR can confer a sensitivity to EGCG at physiologically relevant concentrations, we treated the 67 LR–transfected cells with two concentrations of EGCG (0.1 and 1.0 μM); these concentrations are similar to the amount of EGCG found in human plasma after drinking more than two or three cups of tea[11]. The growth of the transfected cells was inhibited at both of these concentrations (**Fig. 1f**). In addition, this growth-suppressive effect was completely eliminated upon treatment with anti–67 LR before the addition of EGCG. Together, these observations demonstrate that the cell surface 67 LR is the target for EGCG and acts as the receptor for antitumor action of EGCG.

Tea also contains other biologically active compounds such as caffeine[12]. To compare the ability of 67 LR to mediate a response to other tea constituents, we examined caffeine and other tea polyphenols. None of these other compounds affected the growth of 67 LR–expressing cells (**Fig. 2a**), nor could they bind to the cell surface (**Fig. 2b**). EGCG is the only gallate (gallic acid ester) we tested, suggesting that the gallate moiety may be critical for 67 LR binding and subsequent activity.

The recent identification of a role for the 67 LR in retinal angiogenesis and of potent upregulation of this receptor in malignant mesothelioma by gene expression profiling associated with tumor endothelial cells[13] further link this receptor with the anti-angiogenic activities of EGCG. The 67 LR can bind to the prion protein and thus may regulate prion propagation[14]. The fact that EGCG can bind and regulate biological functions of the 67 LR has possible implications for prion-related diseases, for which there is currently no therapy. Ideally, increasing the expression of this target may confer a much higher EGCG potency, similar to the effect of a tumor suppressor gene. Characterizing the mechanisms by which EGCG acts through this 67 LR should help in the design of new strategies to prevent cancer.

Note: Supplementary information is available on the Nature Structural & Molecular Biology website.

ACKNOWLEDGMENTS

We thank T. Shimomura for helpful discussions. We thank M. Sumida and C. Tahara for technical assistance. This work was supported in part by grants from Bio-oriented Technology Research Advancement Institution and from Integrated Research on Safety and Physiological Function of Food, MAFF, Japan, to H.T.

COMPETING INTERESTS STATEMENT

The authors declare that they have no competing financial interests.

Received 15 December 2003; accepted 11 February 2004
Published online at http://www.nature.com/natstructmolbiol/

1. Yang, C.S., Maliakal, P. & Meng, X. *Annu. Rev. Pharmacol. Toxicol.* **42**, 25–54 (2002).
2. Katiyar, S.K. & Mukhtar, H. *Int. J. Oncol.* **8**, 221–238 (1996).
3. Yamane, T. *et al. Cancer Res.* **55**, 2081–2084 (1995).
4. Garbisa, S. *et al. Nat. Med.* **5**, 1216 (1999).
5. Cao, Y. & Cao, R. *Nature* **398**, 381 (1999).
6. Yang, C.S. et al. *Cancer Epidemiol. Biomark. Prev.* **7**, 351–354 (1998).
7. Liang, Y.C., Lin-Shiau, S.Y., Chen, C.F. & Lin, J.K. *J. Cell. Biochem.* **75**, 1–12 (1999).
8. Masuda, M., Suzui, M. & Weinstein, I.B. *Clin. Cancer Res.* **7**, 4220–4229 (2001).
9. Martignone, S. *et al. J. Natl. Cancer Inst.* **85**, 398–402 (1993).
10. Menard, S., Castronovo, V., Tagliabue, E. & Sobel, M.E. *J. Cell. Biochem.* **67**, 155–165 (1997).
11. Yang, C.S. *Nature* **389**, 134–135 (1997).
12. Conlay, L.A., Conant, J.A., deBros, F. & Wurtman, R. *Nature* **389**, 136 (1997).
13. Singhal, S. *et al. Clin. Cancer Res.* **9**, 3080–3097 (2003).
14. Gauczynski, S. *et al. EMBO J.* **20**, 5863–5875 (2001).

Exhibit C

Available online at www.sciencedirect.com
SCIENCE DIRECT®
Biochemical and Biophysical Research Communications 333 (2005) 628–635
BBRC
www.elsevier.com/locate/ybbrc

Epigallocatechin-3-*O*-gallate disrupts stress fibers and the contractile ring by reducing myosin regulatory light chain phosphorylation mediated through the target molecule 67 kDa laminin receptor ☆

Daisuke Umeda, Hirofumi Tachibana *, Koji Yamada

Department of Bioscience and Biotechnology, Faculty of Agriculture, Kyushu University, 6-10-1 Hakozaki, Higashi-ku, Fukuoka 812-8581, Japan

Received 15 May 2005
Available online 31 May 2005

Abstract

Epigallocatechin-3-*O*-gallate (EGCG), a major polyphenol of green tea, has been shown to inhibit the growth of various cancer cell lines. We show here that EGCG induced the disruption of stress fibers and decreased the phosphorylation of the myosin II regulatory light chain (MRLC) at Thr18/Ser19, which is necessary for both contractile ring formation and cell division. Indirect immunofluorescence analysis revealed that EGCG inhibited the concentration of both F-actin and the phosphorylated MRLC in the cleavage furrow at the equator of dividing cells. In addition, EGCG increased the percentages of cells in the G_2/M phase and inhibited cell growth. Recently, we have demonstrated that the anticancer activity of EGCG is mediated by the metastasis-associated 67 kDa laminin receptor (67LR). To explore whether the effect of EGCG is mediated by the 67LR, we transfected cells with short hairpin RNA (shRNA) expression vector to downregulate 67LR expression. When the 67LR was silenced, the suppressive effect of EGCG on the MRLC phosphorylation was significantly attenuated. These results suggest that EGCG inhibits the cell growth by reducing the MRLC phosphorylation and this effect is mediated by the 67LR.

Keywords: Epigallocatechin-3-*O*-gallate; Myosin regulatory light chain; Stress fiber; Contractile ring; 67 kDa laminin receptor

Green tea is a popular beverage worldwide. It has been shown to prevent carcinogenesis in animal models for different organ sites [1]. Many publications suggest that epigallocatechin-3-*O*-gallate (EGCG), the major polyphenol in green tea, is an active compound which has the cancer preventive effects [2–5], however, the molecular mechanism for this inhibitory action is not well understood. Recently, we have reported that the inhibitory effect of EGCG on tumor cell proliferation is exerted by its binding to the 67 kDa laminin receptor (67LR) [6]. The 67LR is expressed on a variety of tumor cells, and expression of this protein is strongly correlated with tumor invasion and metastasis [7,8].

Phosphorylation of the myosin regulatory light chain (MRLC) at Thr18/Ser19 was shown to increase the actin-activated Mg-ATPase activity of myosin II and the assembly of myosin II filaments, and regulate the association between myosin II and filamentous actin (F-actin) [9,10]. The association of myosin II with F-actin results in the formation of stress fibers in interphase cells and the contractile ring in dividing cells [11]. During cytokinesis an actomyosin-based contractile ring is formed at the equator of dividing cells, then gets constricted, and

☆ *Abbreviations:* EGCG, epigallocatechin-3-*O*-gallate; MRLC, myosin regulatory light chain; 67LR, 67 kDa laminin receptor; F-actin, filamentous actin; shRNA, short hairpin RNA; RNAi, RNA interference.

* Corresponding author. Fax: +81 92 642 3008.
E-mail address: tatibana@agr.kyushu-u.ac.jp (H. Tachibana).

0006-291X/$ - see front matter © 2005 Elsevier Inc. All rights reserved.
doi:10.1016/j.bbrc.2005.05.108

finally disappears at the end of cytokinesis [12]. In higher eukaryotes, it is well established that the state of MRLC phosphorylation is cell cycle dependent. During metaphase, the MRLC is phosphorylated predominantly on Ser1/2. However, as the cell cycle progresses through anaphase, the MRLC is dephosphorylated on these sites and is phosphorylated on Ser19 [13,14]. Furthermore, a Ser19-specific biosensor [15], antibodies specific for Ser19 [16], and unphosphorylatable MRLC [17] demonstrate that Ser19 phosphorylation immediately precedes the formation of the cleavage furrow. These findings suggest that myosin II activity is regulated temporally during mitosis, and stimulation of myosin II motor activity by Ser19 phosphorylation could provide the stimulus for the initiation of cytokinesis. On the other hand, the physiological significance of Thr18 phosphorylation is obscure. Nevertheless, it has been demonstrated that the phosphorylation of myosin at Thr18 in addition to Ser19 significantly enhances the actin-activated MgATPase of myosin II and stabilizes the filament formation of myosin II in vitro [18].

Here, we demonstrated that EGCG disrupted the contractile ring through decreasing the MRLC phosphorylation resulting in the inhibition of cell proliferation. Our results suggest that the inhibitory effect of EGCG on the cell growth is based on its ability to reduce the MRLC phosphorylation and is mediated by the cell surface target molecule 67LR.

Materials and methods

Materials and chemicals. Epigallocatechin-3-*O*-gallate (EGCG) was purchased from Kurita Water Industries (Tokyo, Japan). Goat anti-phospho-MRLC (Thr18/Ser19) polyclonal antibody, goat anti-human 67LR polyclonal antibody (F-18), and horseradish peroxidase (HRP)-conjugated anti-goat (donkey) IgG antibody were obtained from Santa Cruz Biotechnology. Rabbit anti-phospho-MRLC (Ser19) polyclonal antibody was purchased from Rockland Immunochemicals. Cy3-conjugated anti-goat IgG antibody was obtained from Chemicon International. Catalase and mouse anti-β-actin antibody were purchased from Sigma. Propidium iodide was obtained from Wako Pure Chemical Industries.

Cell culture and stimulation. HeLa cells were maintained in Dulbecco's modified Eagle's medium (DMEM) (Cosmo Bio, Tokyo, Japan) supplemented with 10% fetal bovine serum (FBS) (Intergen, Purchase, NY), 100 U/ml penicillin G, 100 μg/ml streptomycin, 25 mM Hepes buffer, and 44 mM $NaHCO_3$ in a humidified atmosphere with 5% CO_2 at 37 °C. For some experiments, HeLa cells were plated at a density of 1×10^5 cells/ml. After culturing for 24 h, cells were washed with DMEM. Cells were then incubated at 37 °C with DMEM containing the indicated concentrations of EGCG.

Construction of expression plasmids and transient transfection. The psiRNA-hH1 (G2) short hairpin RNA expression vector was purchased from InvivoGen. As the inserts for expressing short hairpin RNA, three inserts were selected: shRNA1-sense (5′-TCCCGATCT TGACTTCCAGATGGAATTCAAGAGATTCCATCTGGAAGTC AAGATTT-3′) and shRNA1-antisense (5′-CAAAAAATCTT GACTTCCAGATGGAATTCAAGAGTTCCATCTGGAAGTCAA GATC-3′) and shRNA2-sense (5′-TCCCGACCTTCACTAACCAG ATCCATTCAAGAGATTGGATCTGGTTAGTGAAGGTTT-3′) and shRNA2-antisense (5′-CAAAAAACCTTCACTAACCAGAT CCATTCAAGAGATGGATCTGGTTAGTGAAGGTC-3′) and shRNA3-sense (5′-TCCCCGGAGGAATTTCAGGGTGAATTCAA GAGATTCACCCTGAAATTCCTCCTTT-3′) and shRNA3-antisense (5′-CAAAAAAGGAGGAATTTCAGGGTGAATCTCTTGA ATTCACCCTGAAATTCCTCCG-3′). Each insert was annealed and subcloned into psiRNA-hH1 (G2), which was linearized with Bbs I. For transient transfections, HeLa cells were plated in 24-well plates at an approximate density of 2×10^4 cells/ml and cultured for 24 h. FuGENE 6 reagent (Roche, Basel, Switzerland) (0.66 μl/well) was mixed with a total of 333 ng of DNA for 20 min in serum-free medium, then added to the cells in DMEM supplemented with 10% FBS and cultured for 48 or 72 h.

Immunoblotting. After stimulation, the cells were lysed in cell lysis buffer containing 50 mM Tris–HCl (pH 7.5), 150 mM NaCl, 1% Triton-X 100, 1 mM EDTA, 50 mM NaF, 30 mM $Na_4P_2O_7$, 1 mM phenylmethanesulfonyl fluoride (PMSF), 2.0 μg/ml aprotinin, and 1 mM pervanadate. Whole cell lysate was incubated at 4 °C for 30 min and then centrifuged at 15,000*g* for 30 min. The supernatant was mixed with sodium dodecyl sulfate–polyacrylamide gel electrophoresis (SDS–PAGE) sample buffer. The mixture was loaded onto 10% or 12% SDS–PAGE gel, and electrophoresis was done under reducing condition. The sample was then electrotransferred onto a nitrocellulose membrane. The blotted nitrocellulose was probed for phospho-MRLC (Ser19), phospho-MRLC (Thr18/Ser19), and 67LR using the anti-phospho-MRLC (Ser19) antibody, anti-phospho-MRLC (Thr18/Ser19) antibody, and anti-laminin receptor antibody (F-18), respectively. The secondary antibodies used were HRP-conjugated anti-goat IgG or anti-rabbit IgG and detection was done using the ECL kit (Amersham Bioscience, Piscataway, NJ).

Indirect immunofluorescence. HeLa cells were plated at a density of 2×10^4 cells per well in an 8-well glass slide (Nalge Nunc International, Rochester, NY). After stimulation, cells on the glass slide were fixed for 10 min in 3.7% formaldehyde in PBS at room temperature. These fixed cells were made permeable by incubating with 0.2% Triton X-100 in PBS for 5 min and then washed with PBS. After blocking with 1% BSA–PBS, the anti-phospho-MRLC (Thr18/Ser19) antibody was applied directly onto the glass slide and incubated for 1 h at 37 °C. Then, the cells were washed three times with PBS and stained with Cy3-conjugated anti-goat IgG antibody or Alexa Fluor 488 phalloidin (Molecular Probes, Eugene, OR) for 1 h at 37 °C. After washing in PBS, coverslips were mounted onto a glass side with a drop of mounting medium. Imaging was performed with Nikon E600 microscope (Nikon Instech, Kanagawa, Japan). All images were acquired with a digital CCD camera (Nikon Digital Sight DS-5M-L1, Nikon Instech, Kanagawa, Japan) and processed with custom software.

Determination of the cell growth. To assess cell proliferation, cells were plated in 24-well plates at a density of 5×10^4 cells/ml in complete medium. Twenty-four hours after plating, cells were treated with EGCG at the indicated concentrations for the indicated time periods in DMEM supplemented with 2% FBS and 5 mg/ml BSA. For counting, the cells were harvested from triplicate wells with trypsin and counted using a hematometer.

Flow cytometric analysis of the cell cycle. Approximately 3×10^5 HeLa cells were suspended in 300 μl PBS and 700 μl of 100% ethanol was added while vortexing. The cells were incubated at −20 °C for more than 4 h, washed with PBS, and resuspended in 500 μl PBS (pH 8.4) together with 10 μg RNaseA. Incubation was continued at 37 °C for 30 min. The cellular DNA was then stained by applying 500 μl propidium iodide (20 μg/ml) for 30 min at room temperature. The stained cells were analyzed by flow cytometry (FACS Calibur; Becton–Dickinson, Sunnyvale, CA) for relative DNA content. ModFit LT software (Verity Software House, Topsham, ME) was used to assess cell cycle distribution.

Statistical analysis. All values are expressed as means ± SD compared with controls. Statistical analysis was performed by use of Student's *t* test. A level of $p < 0.05$ was considered significant.

Results

Effect of EGCG on cell morphology and actin cytoskeleton organization in HeLa cells

To examine the effect of EGCG on cell morphology and actin cytoskeleton, we stained HeLa cells for F-actin with Alexa Fluor 488 phalloidin. Control HeLa cells exhibited an organized network of F-actin containing stress fibers spanning across the cell body and a thin cortical F-actin rim at the margins (Fig. 1A). This rim was so thin that cell–cell junctions were not distinguishable. When the cells were incubated with the indicated concentrations of EGCG for 20 min, the cells retracted and left intercellular gaps (Fig. 1A). In addition, disappearance of the stress fibers in the central cell body was observed upon treatment with EGCG, and the peripheral actin rim became thicker, providing an outline of the cell–cell junctions (Fig. 1A). When treated with 50 μM EGCG, actin cytoskeletal remodeling was observed even at a time point of 1 min (Fig. 1B). This effect continued for at least 10 min.

Effect of EGCG on Thr18/Ser19 phosphorylation of MRLC

Because stress fiber formation has been known to require Thr18/Ser19 phosphorylation of MRLC [11], we examined the effect of EGCG on the MRLC phosphorylation by Western blot analysis using phosphorylated MRLC-specific antibodies. EGCG dose-dependently decreased the diphosphorylation of MRLC at Thr18/Ser19 (Fig. 2A, top). Monophosphorylation of MRLC at Ser19 is sufficient to stimulate actin-activated myosin II Mg-ATPase [19]. EGCG also decreased the monophosphorylation at Ser19 in a dose-dependent manner (Fig. 2A, middle). EGCG clearly reduced the phosphorylation at 1 min and this effect continued for at least 10 min (Fig. 2B). These results correlate well with EGCG-induced actin cytoskeleton remodeling as shown in Fig. 1.

EGCG has been reported to inhibit cancer cell proliferation directly by affecting the signaling pathway involved in cell growth [20,21]. However, the concentration range of EGCG shown to have an effect (20–100 μM) in previous studies is much higher than that observed in blood or tissues. To investigate whether the physiologically relevant concentrations of EGCG can reduce the MRLC phosphorylation, we treated HeLa cells for 24 h with three concentrations of EGCG (0.1, 1 or 10 μM); these concentrations are similar to the amount of EGCG found in human plasma after drinking more than two or three cups of tea [22]. The MRLC phosphorylation was reduced at concentrations between 1 and 10 μM (Fig. 2C).

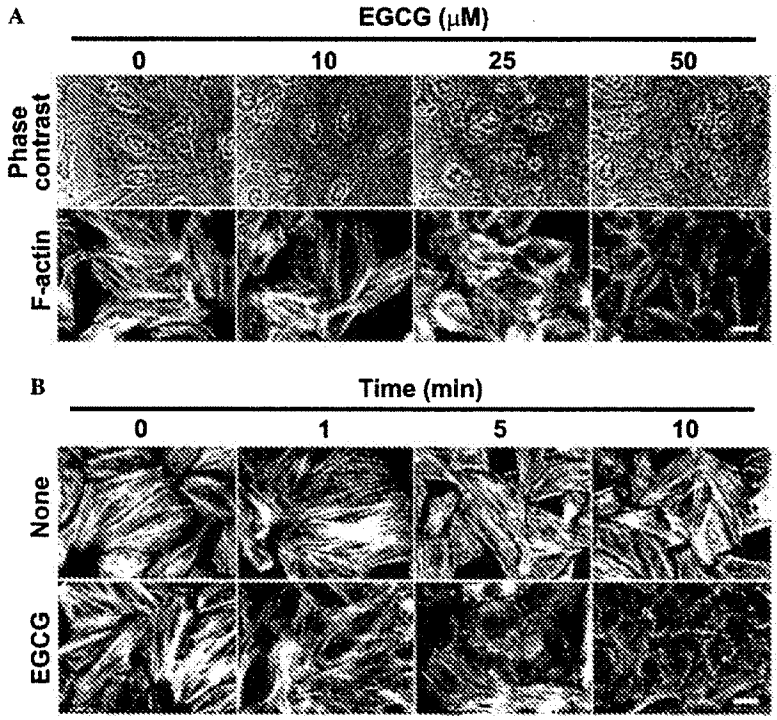

Fig. 1. Effect of EGCG on cell morphology and actin cytoskeleton organization in HeLa cells. HeLa cells were plated at a density of 2×10^4 cells per well in an 8-well glass slide in DMEM supplemented with 10% FBS and cultured for 24 h. The cells were treated with the indicated concentrations of EGCG for 20 min in DMEM (A) or treated with 50 μM EGCG for the indicated time periods (B). Cells were then fixed and stained with Alexa Fluor 488 phalloidin. The bar represents 30 μm.

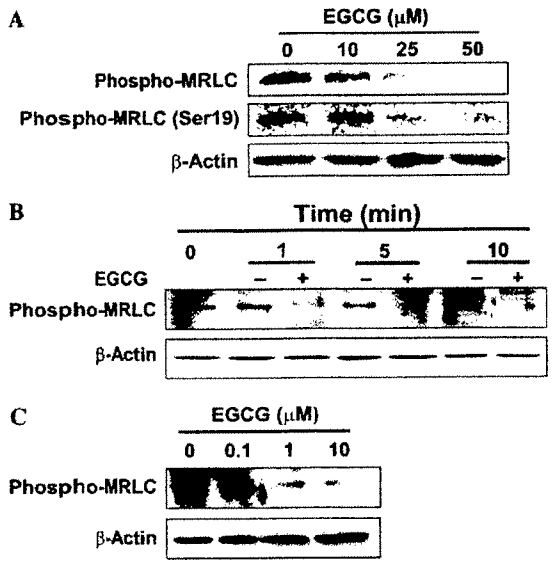

Fig. 2. Effect of EGCG on Thr18/Ser19 phosphorylation of MRLC. (A) HeLa cells were plated at a density of 1×10^5 cells/ml in DMEM supplemented with 10% FBS and cultured for 24 h. Cells were then treated with the indicated concentrations of EGCG for 20 min in DMEM and total cellular protein was subjected to Western blot analysis using an anti-phospho-MRLC (Thr18/Ser19) antibody (top) or anti-phospho-MRLC (Ser19) antibody (middle). HeLa cells were plated at a density of 1×10^5 cells/ml in DMEM supplemented with 10% FBS and cultured for 24 h. The cells were treated with 50 μM EGCG for the indicated time periods (B) or treated with the indicated concentrations of EGCG in DMEM for 24 h (C). Total cellular protein was then subjected to Western blot analysis using an anti-phospho-MRLC (Thr18/Ser19) antibody.

Effect of EGCG on the concentration of F-actin and the phosphorylated MRLC in the cleavage furrow at the equator of dividing cells

The phosphorylation of MRLC at Thr18/Ser19 has been shown to be necessary for formation of the contractile ring in dividing cells [11]. To examine the effect of EGCG on contractile ring formation, HeLa cells were treated with 50 μM EGCG for 10 min and stained for F-actin. At low magnification (Fig. 3A), the contractile ring in dividing cells not treated with EGCG exhibited spot-like aggregated F-actin (indicated by arrowheads). However, in EGCG-treated cells these spot-like F-actin condensations disappeared and the cell peripheral actin rim was able to be visualized. We then double stained the dividing cells for F-actin and the phosphorylated MRLC utilizing Alexa Fluor 488 phalloidin and the phospho-MRLC (Thr18/Ser19) specific antibody, respectively. As shown in Fig. 3B, at high magnification it is clearly observed that EGCG inhibited the assembly of F-actin and the phosphorylation of MRLC in the cleavage furrow of dividing cells (indicated by arrows).

Effect of EGCG on the growth and cell cycle

We next examined the effect of EGCG on the growth and cell cycle of HeLa cells. Treatment of the cells with 50 μM EGCG inhibited cell growth (Fig. 4A) and significantly reduced not only the diphosphorylation of MRLC at Thel8/Ser19 (Fig. 4B, top) but also the monophosphorylation at Ser19 (Fig. 4B, middle).

Given that EGCG inhibited the contractile ring formation by reducing the MRLC phosphorylation and thus inhibited the cell growth, to determine if EGCG treatment could alter the cell cycle, we subjected EGCG-treated cells to FACS analysis using propidium iodide staining to measure the DNA content. EGCG treatment for 48 h significantly increased the percentage of cells in the G_2/M phase (Fig. 4C). These results suggest that the suppressive effect of EGCG on the MRLC phosphorylation continued at least for 48 h and the increase of G_2/M phase cells resulted from the effect of EGCG.

EGCG-induced reduction of the MRLC phosphorylation is not affected by catalase

EGCG has been known to produce H_2O_2 when it is added to the media of several cultured cell lines, and H_2O_2 may exert biological effects on cell growth. It has been reported that 30 μM EGCG can induce apoptosis in H661 lung cancer cells, and this effect could be abolished by the addition of catalase (50 U/ml) in the culture medium [23]. We examined whether catalase can change the effect of EGCG on cell growth and MRLC phosphorylation. The addition of catalase could not alter the EGCG-induced reduction of the MRLC phosphorylation level (Fig. 5A), the inhibition of the cell growth (Fig. 5B) or the accumulation of the cells in G_2/M phase (Fig. 5C).

Effect of 67LR-downregulation on the EGCG-induced reduction of the MRLC phosphorylation

Recently, we have identified the 67LR as a cell surface receptor that mediates the anticancer activity of EGCG [6]. We hypothesized that if EGCG exerts its effect by binding to the cell surface 67LR, the effect would be affected by the removal of EGCG. To assess the reversibility of the EGCG-induced reduction of the MRLC phosphorylation, cells were treated with or without 50 μM EGCG. After a 20 min treatment, the cells were transferred to an EGCG-free medium and incubated for 360 min. As shown in Fig. 6A, the removal of EGCG restored the MRLC phosphorylation to a level similar to that observed in untreated cultures. This recovery of the MRLC phosphorylation might be due to the dissociation of EGCG from 67LR. To analyze whether the suppressive effect of EGCG on the MRLC

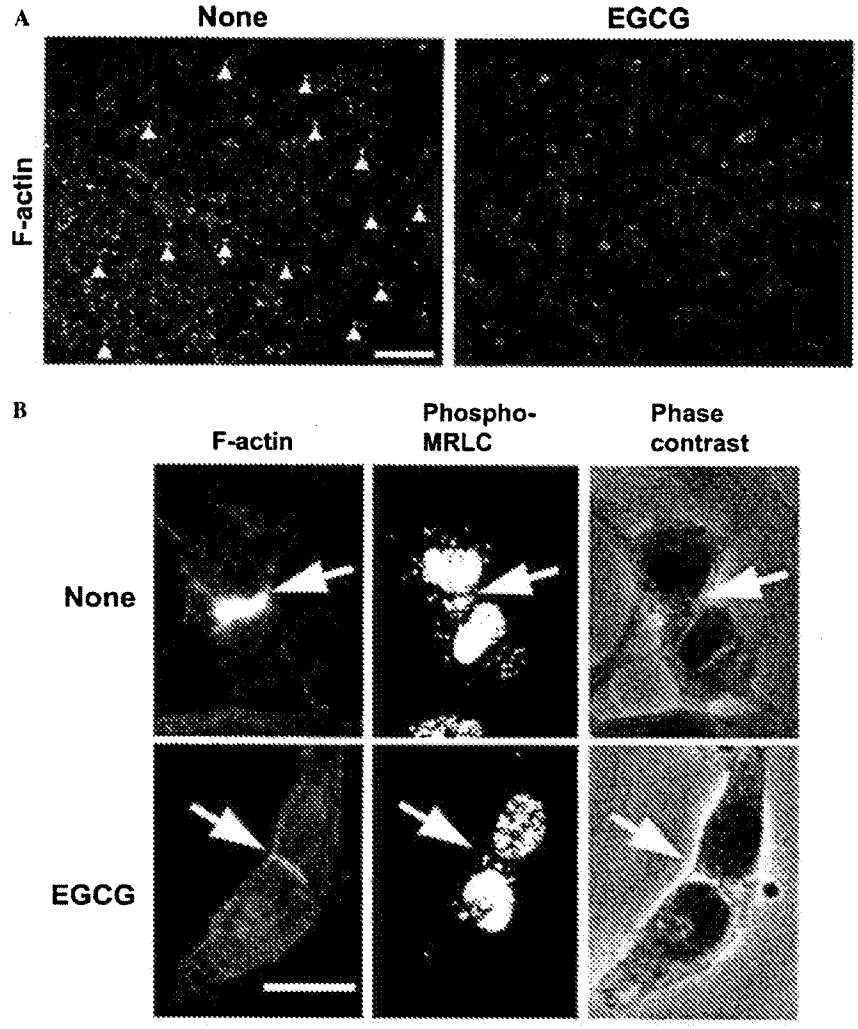

Fig. 3. Effect of EGCG on the concentration of F-actin and the phosphorylated MRLC in the cleavage furrow at the equator of dividing cells. HeLa cells were plated at a density of 2×10^4 cells per well in an 8-well glass slide in DMEM supplemented with 10% FBS and cultured for 24 h. The cells were treated with 50 μM EGCG for 10 min in DMEM. The cells were fixed and stained with Alexa Fluor 488 phalloidin and anti-phospho-MRLC (Thr18/Ser19) antibody. The bar in (A) and (B) represents 100 and 20 μm, respectively.

phosphorylation is mediated by the 67LR, RNA interference (RNAi)-mediated gene silencing was utilized to knock down the expression of the 67LR. HeLa cells were transiently transfected with three short hairpin RNA (shRNA) expression vectors for the 67LR. The 67LR silencing was observed when each of the shRNA expression vectors was trasnsfected separately (data not shown), however when we combined all three shRNA expression vectors, the highest silencing was observed (Fig. 6B). We confirmed the elimination of the EGCG inhibitory effect on the growth of cells transfected with all three shRNA expression vectors (Fig. 6C). Fig. 6D shows that 25 μM EGCG significantly reduced the monophosphorylation of MRLC at Ser19 in the cells transfected with the empty vector, however in the cells transfected with shRNA expression vectors for the 67LR, the same concentration of EGCG only slightly reduced the phosphorylation. These results suggest that 67LR does indeed mediate the suppressive effect of EGCG on MRLC phosphorylation.

Discussion

Here, we demonstrate that EGCG decreased MRLC phosphorylation at Thr18/Ser19 and disrupted the stress fibers and contractile ring. Further EGCG-induced cell growth-inhibition and accumulation of the cells in G_2/M phase correlated with the suppressive effect of EGCG on the MRLC phosphorylation.

The F-actin staining revealed that EGCG disrupted stress fibers and inhibited the assembly of F-actin in the cleavage furrow at the equator of dividing cells. Because the MRLC phosphorylation has been shown to be necessary for the assembly of stress fibers in interphase cells and the formation of contractile ring in dividing

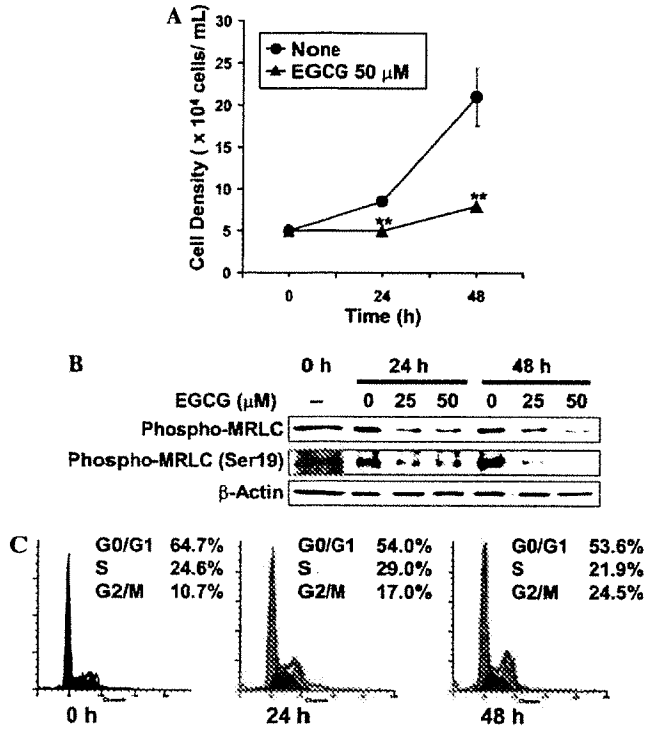

Fig. 4. Effect of EGCG on the growth and the cell cycle. (A) Cells were counted after treatment with or without 50 μM EGCG in DMEM supplemented with 2% FBS and 5 mg/ml BSA for the indicated time periods. Data shown are means ± SD for three samples. Data containing asterisk marks are significantly different from the values in control at $^{**}p < 0.01$. (B) Measurement of the level of MRLC phosphorylation. Cells were treated with 25 or 50 μM EGCG in DMEM supplemented with 2% FBS and 5 mg/ml BSA for the indicated time periods. Total cellular protein was subjected to Western blot analysis using an anti-phospho-MRLC (Thr18/Ser19) antibody (top) or anti-phospho-MRLC (Ser19) antibody (middle). (C) FACS analysis of the cell cycle. Cells were treated with 50 μM EGCG for the indicated time periods and then evaluated for DNA content after propidium iodide staining.

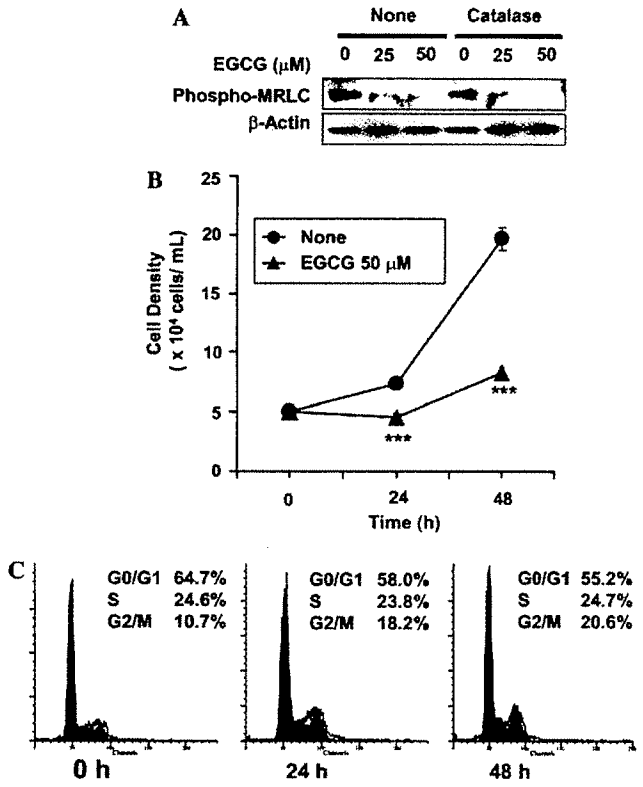

Fig. 5. Effect of catalase on the activities of EGCG. (A) HeLa cells were plated at a density of 1×10^5 cells/ml in DMEM supplemented with 10% FBS and cultured for 24 h. Cells were then treated with the indicated concentrations of EGCG and 200 U/ml catalase for 20 min in DMEM. Total cellular protein was subjected to Western blot analysis using an anti-phospho-MRLC (Thr18/Ser19) antibody. (B) Cell number was determined after treatment with 50 μM EGCG in DMEM supplemented with 2% FBS, 5 mg/ml BSA, and 200 U/ml catalase for the indicated time periods. Data shown are means ± SD for three samples. Data containing asterisk marks are significantly different from the values in control at $^{***}p < 0.001$. (C) FACS analysis of the cell cycle. Cells were treated with 50 μM EGCG in DMEM supplemented with 2% FBS, 5 mg/ml BSA, and 200 U/ml catalase for the indicated time periods, and then evaluated for DNA content after propidium iodide staining.

cells [11], we suggest that the effects of EGCG on the actin cytoskeleton are due to an EGCG-induced decrease of the MRLC phosphorylation level.

Many studies have demonstrated that EGCG has an important antiproliferative effect against certain cancers, including lung, bronchial, colon, prostate, breast, liver, and leukemia cancer cells [2]. Although the mode of action of EGCG on tumor cell growth inhibition is mainly related to the blockage of the cell cycle progression, the phase in which cells are arrested by EGCG is dependent on the cell type [24,25]. In this study, EGCG treatment resulted in the accumulation of HeLa cells in the G_2/M phase.

In higher eukaryotes, phosphorylation of MRLC on specific residues varies with time during mitosis. During metaphase, the MRLC is phosphorylated predominantly on Ser1/2, which has an inhibitory effect on myosin II's ATPase activity. However, by anaphase, MRLC is dephosphorylated on these sites and is phosphorylated on Ser19, which stimulates the motor and perhaps the assembly properties of myosin II [13,14,17]. These observations indicate that myosin II activity is regulated temporally during mitosis, and suggests that MRLC phosphorylation on Ser19 could provide the stimulus for contraction of the cleavage furrow. Inhibition of the myosin phosphatase and activation of MLCK during the later stages of mitosis would favor increased levels of Ser19 phosphorylation and the activation of myosin II motor activity required for cytokinesis [26]. We suggest that EGCG inhibited the cytokinesis by reducing the level of MRLC phosphorylation and inhibiting the concentration of the phosphorylated MRLC in the cleavage furrow. This is supported by the observation that EGCG-treatment leads to the accumulation of cells in G_2/M phase and a report stating that

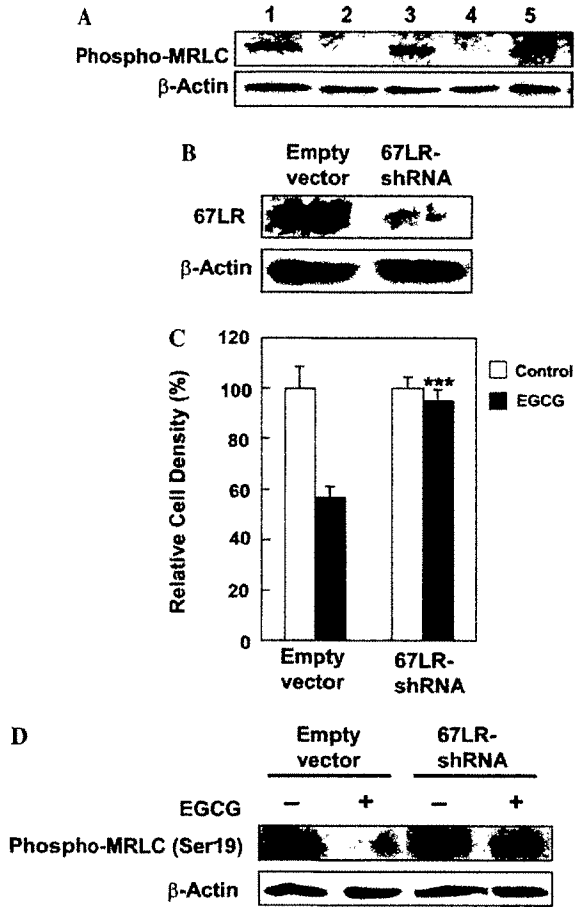

Fig. 6. Effect of 67LR-downregulation on the EGCG-induced reduction of the MRLC phosphorylation. (A) Cells were treated with (lanes 2 and 4) or without 50 μM EGCG (lanes 1 and 3) in DMEM for 20 min (lanes 1 and 2) or 380 min (lanes 3 and 4). The cells were treated with 50 μM EGCG for 20 min in DMEM and then treated for 360 min in EGCG-free DMEM (lane 5). Then total cellular protein was subjected to Western blot analysis using an anti-phospho-MRLC (Thel8/Ser19) antibody. (B) Measurement of the 67LR expression level in HeLa cells transiently transfected with shRNA expression vector targeting the 67LR mRNA. Total cellular protein was subjected to Western blot analysis using an anti-67LR antibody (F-18). (C) The cells were plated at a density of 1×10^4 cells/ml in DMEM supplemented with 10% FBS and cultured for 24 h. Cells were then transiently transfected with the shRNA expression vectors targeting the 67LR mRNA and cultured for 48 h in DMEM supplemented with 10% FBS. The cells were treated with 25 μM EGCG in DMEM supplemented with 2% FBS and 5 mg/ml BSA for 96 h. Data shown are means ± SD for three samples. Data containing asterisk marks are significantly different from the values in empty vector at $^{***}p < 0.001$. (D) The cells were plated at a density of 2×10^4 cells/ml in DMEM supplemented with 10% FBS and cultured for 24 h. Then cells were transiently transfected with the above shRNA expression vector and cultured for 72 h in DMEM supplemented with 10% FBS. The cells were treated with 25 μM EGCG in DMEM for 20 min. Then total cellular protein was subjected to Western blot analysis using an anti-phospho-MRLC (Ser19) antibody.

unphosphorylatable MRLC overexpression resulted in the production of multinucleated cells [17].

EGCG can generate H_2O_2 [27,28], and H_2O_2 can exert biological effects on cells [29,30]. Therefore, results from in vitro studies with EGCG, especially at high concentrations, should be interpreted with caution to clearly distinguish between the direct effects of EGCG- and H_2O_2-mediated effects. Our experiments here show that catalase could not alter any of the EGCG-induced effects on cell proliferation or the MRLC phosphorylation, indicating that the effects of EGCG are not due to the production of H_2O_2.

Previously, we reported that EGCG exerts an inhibitory effect on cell growth by binding to the 67LR [6], however, the precise mechanism for this action, especially after EGCG binds to the 67LR, was entirely unknown. In this study, we showed that the suppressive action of EGCG on the MRLC phosphorylation is blocked by downregulation of 67LR. We suggest that EGCG-induced reduction of the MRLC phosphorylation is involved in signal transduction pathways that is mediated post EGCG binding to 67LR. Plasma EGCG concentrations after ingestion of green tea in humans lie within 1 μM [31,32]. Although the concentrations of EGCG in our cell culture model are above this value, we observed here that treatment with 1 μM EGCG for 24 h reduced the MRLC phosphorylation in HeLa cells. Because the MRLC phosphorylation regulates many cellular functions, these findings may lead to a better understanding of mechanisms involved in the various biological effects of EGCG in vivo.

Acknowledgments

This work was supported in part by Grants from Research and Development Program for New Bio-industry Initiatives (to H.T.). The authors thank Dr. T. Shimomura for helpful discussions and Perry Seto for proofreading the manuscript.

References

[1] I.E. Dreosti, M.J. Wargovich, C.S. Yang, Inhibition of carcinogenesis by tea: the evidence from experimental studies, Crit. Rev. Food Sci. Nutr. 37 (1997) 761–770.
[2] C.S. Yang, P. Maliakal, X. Meng, Inhibition of carcinogenesis by tea, Annu. Rev. Pharmacol. Toxicol. 42 (2002) 25–54.
[3] J.Y. Chung, C. Huang, X. Meng, Z. Dong, C.S. Yang, Inhibition of activator protein 1 activity and cell growth by purified green tea and black tea polyphenols in H-ras-transformed cells: structure–activity relationship and mechanisms involved, Cancer Res. 59 (1999) 4610–4617.
[4] M. Isemura, K. Saeki, T. Minami, S. Hayakawa, T. Kimura, Y. Shoji, M. Sazuka, Inhibition of matrix metalloproteinases by tea catechins and related polyphenols, Ann. N.Y. Acad. Sci. 878 (1999) 629–631.
[5] K. Saeki, S. Hayakawa, M. Isemura, T. Miyase, Importance of a pyrogallol-type structure in catechin compounds for apoptosis-inducing activity, Phytochemistry 53 (2000) 391–394.
[6] H. Tachibana, K. Koga, Y. Fujimura, K. Yamada, A receptor for green tea polyphenol EGCG, Nat. Struct. Mol. Biol. 11 (2004) 380–381.

[7] S. Martignone, S. Menard, R. Bufalino, N. Cascinelli, R. Pellegrini, E. Tagliabue, S. Andreola, F. Rilke, M.I. Colnaghi, Prognostic significance of the 67-kilodalton laminin receptor expression in human breast carcinomas, J. Natl. Cancer Inst. 85 (1993) 398–402.
[8] S. Menard, V. Castronovo, E. Tagliabue, M.E. Sobel, New insights into the metastasis-associated 67 kD laminin receptor, J. Cell. Biochem. 67 (1997) 155–165.
[9] Z.M. Goeckeler, R.B. Wysolmerski, Myosin light chain kinase-regulated endothelial cell contraction: the relationship between isometric tension, actin polymerization, and myosin phosphorylation, J. Cell Biol. 130 (1995) 613–627.
[10] M. Ikebe, S. Reardon, Phosphorylation of bovine platelet myosin by protein kinase C, Biochemistry 29 (1990) 2713–2720.
[11] T. Iwasaki, M. Murata-Hori, S. Ishitobi, H. Hosoya, Diphosphorylated MRLC is required for organization of stress fibers in interphase cells and the contractile ring in dividing cells, Cell Struct. Funct. 26 (2001) 677–683.
[12] M. Glotzer, Animal cell cytokinesis, Annu. Rev. Cell Dev. Biol. 17 (2001) 351–386.
[13] L.L. Satterwhite, M.J. Lohka, K.L. Wilson, T.Y. Scherson, L.J. Cisek, J.L. Corden, T.D. Pollard, Phosphorylation of myosin-II regulatory light chain by cyclin-p34cdc2: a mechanism for the timing of cytokinesis, J. Cell Biol. 118 (1992) 595–605.
[14] Y. Yamakita, S. Yamashiro, F. Matsumura, In vivo phosphorylation of regulatory light chain of myosin II during mitosis of cultured cells, J. Cell Biol. 124 (1994) 129–137.
[15] R.L. DeBiasio, G.M. LaRocca, P.L. Post, D.L. Taylor, Myosin II transport, organization, and phosphorylation: evidence for cortical flow/solation-contraction coupling during cytokinesis and cell locomotion, Mol. Biol. Cell 7 (1996) 1259–1282.
[16] F. Matsumura, S. Ono, Y. Yamakita, G. Totsukawa, S. Yamashiro, Specific localization of serine 19 phosphorylated myosin II during cell locomotion and mitosis of cultured cells, J. Cell Biol. 140 (1998) 119–129.
[17] S. Komatsu, T. Yano, M. Shibata, R.A. Tuft, M. Ikebe, Effects of the regulatory light chain phosphorylation of myosin II on mitosis and cytokinesis of mammalian cells, J. Biol. Chem. 275 (2000) 34512–34520.
[18] M. Ikebe, J. Koretz, D.J. Hartshorne, Effects of phosphorylation of light chain residues threonine 18 and serine 19 on the properties and conformation of smooth muscle myosin, J. Biol. Chem. 263 (1988) 6432–6437.
[19] M. Ikebe, D.J. Hartshorne, Phosphorylation of smooth muscle myosin at two distinct sites by myosin light chain kinase, J. Biol. Chem. 260 (1985) 10027–10031.
[20] Y.C. Liang, S.Y. Lin-Shiau, C.F. Chen, J.K. Lin, Inhibition of cyclin-dependent kinases 2 and 4 activities as well as induction of Cdk inhibitors p21 and p27 during growth arrest of human breast carcinoma cells by (−)-epigallocatechin-3-gallate, J. Cell. Biochem. 75 (1999) 1–12.
[21] M. Masuda, M. Suzui, J.T. Lim, I.B. Weinstein, Effects of epigallocatechin-3-gallate on growth, epidermal growth factor receptor signaling pathways, gene expression, and chemosensitivity in human head and neck squamous cell carcinoma cell lines, Clin. Cancer Res. 7 (2001) 4220–4229.
[22] C.S. Yang, Inhibition of carcinogenesis by tea, Nature 389 (1997) 134–135.
[23] G.Y. Yang, J. Liao, K. Kim, E.J. Yurkow, C.S. Yang, Inhibition of growth and induction of apoptosis in human cancer cell lines by tea polyphenols, Carcinogenesis (Lond.) 19 (1998) 611–616.
[24] A. Chen, L. Zhang, J. Xu, J. Tang, The antioxidant (−)-epigallocatechin-3-gallate inhibits activated hepatic stellate cell growth and suppresses acetaldehyde-induced gene expression, Biochem. J. 368 (2002) 695–704.
[25] H. Fujiki, M. Suganuma, S. Okabe, N. Sueoka, A. Komori, E. Sueoka, T. Kozu, Y. Tada, K. Suga, K. Imai, K. Nakachi, Cancer inhibition by green tea, Mutat. Res. 402 (1998) 307–310.
[26] A. Poperechnaya, O. Varlamova, P. Lin, J.T. Stull, A.R. Bresnick, Localization and activity of myosin light chain kinase isoforms during the cell cycle, J. Cell Biol. 151 (2000) 697–707.
[27] J. Hong, H. Lu, X. Meng, J.H. Ryu, Y. Hara, C.S. Yang, Stability, cellular uptake, biotransformation, and efflux of tea polyphenol (−)-epigallocatechin-3-gallate in HT-29 human colon adenocarcinoma cells, Cancer Res. 62 (2002) 7241–7246.
[28] J.Z. Shen, X.F. Zheng, E.Q. Wei, C.Y. Kwan, Green tea catechins evoke a phasic contraction in rat aorta via H_2O_2-mediated multiple-signalling pathways, Clin. Exp. Pharmacol. Physiol. 30 (2003) 88–95.
[29] H. Arakawa, M. Maeda, S. Okubo, T. Shimamura, Role of hydrogen peroxide in bactericidal action of catechin, Biol. Pharm. Bull. 27 (2004) 277–281.
[30] S.R. Thomas, K. Chen, J.F. Keaney Jr., Hydrogen peroxide activates endothelial nitric-oxide synthase through coordinated phosphorylation and dephosphorylation via a phosphoinositide 3-kinase-dependent signaling pathway, J. Biol. Chem. 277 (2002) 6017–6024.
[31] C.S. Yang, L. Chen, M.J. Lee, D. Balentine, M.C. Kuo, S.P. Schantz, Blood and urine levels of tea catechins after ingestion of different amounts of green tea by human volunteers, Cancer Epidemiol. Biomarkers Prev. 7 (1998) 351–354.
[32] K. Umegaki, A. Sugisawa, K. Yamada, M. Higuchi, Analytical method of measuring tea catechins in human plasma by solid-phase extraction and HPLC with electrochemical detection, J. Nutr. Sci. Vitaminol. 47 (2001) 402–408.

Exhibit D

Specific killing of multiple myeloma cells by (–)-epigallocatechin-3-gallate extracted from green tea: biologic activity and therapeutic implications

Masood A. Shammas, Paola Neri, Hemanta Koley, Ramesh B. Batchu, Robert C. Bertheau, Vidit Munshi, Rao Prabhala, Mariateresa Fulciniti, Yu tzu Tai, Steven P. Treon, Raj K. Goyal, Kenneth C. Anderson, and Nikhil C. Munshi

Epigallocatechin-3-gallate (EGCG), a polyphenol extracted from green tea, is an antioxidant with chemopreventive and chemotherapeutic actions. Based on its ability to modulate growth factor–mediated cell proliferation, we evaluated its efficacy in multiple myeloma (MM). EGCG induced both dose- and time-dependent growth arrest and subsequent apoptotic cell death in MM cell lines including IL-6–dependent cells and primary patient cells, without significant effect on the growth of peripheral blood mononuclear cells (PBMCs) and normal fibroblasts. Treatment with EGCG also led to significant apoptosis in human myeloma cells grown as tumors in SCID mice. EGCG interacts with the 67-kDa laminin receptor 1 (LR1), which is significantly elevated in myeloma cell lines and patient samples relative to normal PBMCs. RNAi-mediated inhibition of LR1 resulted in abrogation of EGCG-induced apoptosis in myeloma cells, indicating that LR1 plays an important role in mediating EGCG activity in MM while sparing PBMCs. Evaluation of changes in gene expression profile indicates that EGCG treatment activates distinct pathways of growth arrest and apoptosis in MM cells by inducing the expression of death-associated protein kinase 2, the initiators and mediators of death receptor–dependent apoptosis (Fas ligand, Fas, and caspase 4), p53-like proteins (p73, p63), positive regulators of apoptosis and NF-κB activation (CARD10, CARD14), and cyclin-dependent kinase inhibitors (p16 and p18). Expression of related genes at the protein level were also confirmed by Western blot analysis. These data demonstrate potent and specific antimyeloma activity of EGCG and provide the rationale for its clinical evaluation. (Blood. 2006;108:2804-2810)

Introduction

Tea leaves, derived from a shrub *Camellia sinensis*, contain high amounts of polyphenols or catechins. During the extraction process, the polyphenols in black tea are rendered inactive by fermentation; however, the extraction process for green tea involves only steaming and thus leaves the polyphenols active.[1]

In recent years, chemopreventive and chemotherapeutic effects of green tea have been reported in different malignancies.[2-9] Because epigallocatechin-3-gallate (EGCG) is the most abundant and biologically active polyphenol with antioxidant activity in green tea, the majority of the mechanistic studies have focused on this compound. It selectively inhibits cell growth and induces apoptosis in cancer cells without adversely affecting normal cells.[10] The antitumor effects of EGCG include inhibition of angiogenesis, modulation of growth factor–mediated proliferation, suppression of oxidative damage, induction of apoptosis, and cell-cycle arrest.[8,11-14] Both epidemiologic studies on tea consumption[15,16] and animal studies[6,17] have shown that the polyphenols prevent the development of chemically induced cancer.

Cell growth inhibition and apoptosis-inducing effects of EGCG have been shown in several cancers.[18,19] In prostate carcinoma cells (LNcaP), EGCG induces apoptosis by activation of p53 and p14ARF-mediated suppression of MDM2. In this study we have demonstrated that EGCG induces apoptotic cell death in multiple myeloma (MM) cells including IL-6–dependent cells and primary MM cells in vitro, while having no significant effect on growth of normal cells (peripheral blood mononuclear cells [PBMCs] and fibroblasts), and induces apoptosis and inhibition of growth in vivo in a murine model of human MM. Antimyeloma effects of EGCG are mediated through laminin receptor 1 (LR1), which is overexpressed on MM cells, and it activates multiple interrelated pathways of apoptosis and cell-cycle arrest.

Materials and methods

Chemicals

(–)-Epigallocatechin-3-gallate (EGCG) was purchased from Sigma-Aldrich (St Louis, MO) and dissolved in phosphate-buffered saline (PBS).

MM and normal cells

The MM cell line INA6 was kindly provided by Dr Renate Burger (University of Erlangen-Nuernberg, Erlangen, Germany) and the ARP cell line was kindly provided by Dr J. Epstein (University of Arkansas for Medical Sciences, Little Rock). Normal diploid fibroblasts (GM07675)

From the Veterans Administration (VA) Boston Health Care System and Dana Farber Cancer Institute, Harvard Medical School, Boston, MA.

Submitted December 21, 2005; accepted June 14, 2006. Prepublished online as *Blood* First Edition Paper, June 29, 2006; DOI 10.1182/blood-2006-05-022814.

Supported in part by National Institutes of Health (NIH) grant DK031092, a Merit Review Award from the Research Service Veterans Health Care (VHA) (R.K.G.), NIH-P50-100007 Developmental Research Award (M.A.S.), a Merit Review Award from the Research Service, a Merit Review Award from Epidemiology Service VHA (N.C.M.), and NIH-P050-100007 and NIH-PO1-78378 (N.C.M. and K.C.A.). N.C.M. is a Leukemia Society Scholar in Translational Research.

Reprints: Nikhil C. Munshi, Dana Farber Cancer Institute, 44 Binney St, D1B25, Boston, MA 02115; e-mail: nikhil_munshi@dfci.harvard.edu.

The publication costs of this article were defrayed in part by page charge payment. Therefore, and solely to indicate this fact, this article is hereby marked "advertisement" in accordance with 18 U.S.C. section 1734.

were obtained from the American Type Culture Collection (Rockville, MD). ARP cells were cultured in RPMI 1640 medium supplemented with 10% fetal bovine serum (HyClone, South Logan, UT), whereas INA6, an interleukin 6 (IL-6)–dependent cell line, was cultured in RPMI 1640 medium supplemented with 20% fetal bovine serum (HyClone) and 2.5 ng/mL recombinant human IL-6 (R&D Systems, Minneapolis, MN). Normal diploid fibroblasts (GM07675) were cultured in Dulbecco modified Eagle medium (DMEM; Sigma-Aldrich) containing 10% fetal bovine serum. All cell lines were maintained in a state of logarithmic growth at 37°C in humidified air with 5% CO_2, as described previously.[20-23] For RNA and protein analyses, cultures were harvested at the same final cell density (5×10^5/mL) and immediately processed.

Primary MM cells were isolated from bone marrow aspirate samples, obtained following informed consent, obtained in accordance with the Declaration of Helsinki, from patients with MM, by positive selection using anti-CD138 antibody-coated immunomagnetic beads and magnetic-assisted cell sorting (MACS), according to the manufacturer's instructions (Miltenyi Biotech, Auburn, CA). Purity of plasma cells (> 95%) was confirmed by monitoring cell-surface expression of CD38 and CD45.

Treatment and growth of cells

Cells (5×10^5) were plated in 100-mm dishes and treated with EGCG at various concentrations and live cell number was determined by trypan blue exclusion or by measuring ^{3}H-thymidine incorporation on alternate days. For thymidine incorporation, 2×10^4 cells/well were incubated in 96-well culture plates with or without EGCG in triplicate. ^{3}H-thymidine (0.5 μCi [0.0185 MBq]; NEN Life Science Products, Boston, MA) was then added to each well for the last 8 hours. Cells were harvested onto glass filters with an automatic cell harvester (Cambridge Technology, Cambridge, MA), and ^{3}H-thymidine uptake was measured using a Micro-Beta Trilux counter (Wallac, Gaithersburg, MD).

siRNA and transfections

Nontargeting Cy3-labeled control siRNA and siRNA targeting LR1 (67 kDa) were purchased from Dharmacon Research (Lafayette, CO). siRNAs were transfected into MM cells using *Trans*IT-TKO transfection reagent (Mirus, Madison, WI), as described by the manufacturer. Briefly, cells were plated at 2×10^5/mL in complete growth medium 24 hours prior to transfection and incubated overnight. Immediately prior to transfection, *Trans*IT-TKO reagent was added dropwise to serum-free medium (RPMI 1640) and incubated at room temperature for 20 minutes. siRNA duplexes (100 nM) were added to diluted *Trans*IT-TKO reagent, mixed, and incubated at room temperature for 20 minutes. siRNA-TKO complexes were then layered dropwise onto the cells and incubated as described.[24,25]

To monitor uptake of siRNA, cells transfected with Cy3-labeled control siRNA were incubated for 72 hours and Cy3 labeling was examined using an Olympus BX61 fluorescence microscope (Olympus America, Center Valley, PA) equipped with a Cy3 filter and a UPlanApo Olympus 20×/0.70 numeric aperture objective. Images were photographed using a SPOT RT color 2.2.1 digital camera (Diagnostic Instruments, Sterling Heights, MI), and were acquired using SPOT 3.4.2 image software (Diagnostic Instruments).

Animals

SCID mice (CB-17), obtained from Taconic (Germantown, NY), were maintained and monitored in the Farber Cancer Institute's Animal Research Facility. All animal studies were conducted according to protocols approved by the Institutional Animal Care and Use Committee. Animals were humanely killed when their tumors reached 2 cm in diameter or when paralysis or major compromise in their quality of life occurred.

Human MM xenograft murine model

CB-17 SCID mice were inoculated subcutaneously in the interscapular area with 2.5×10^6 OPM1 cells in 100 μL RPMI 1640 medium. Following appearance of palpable tumors, mice were injected intraperitoneally daily with PBS alone or EGCG (33 mg/kg). At the time of the animals' death, tumors were excised and cell-cycle profiles of tumor cells derived from control and EGCG-treated mice were analyzed using propidium iodide (PI) staining and flow cytometry. Briefly, cells (1×10^6) were washed with PBS, permeabilized by a 30-minute exposure to cold 70% ethanol at 4°C, washed with PBS, incubated with PI (5 μg/mL) in 500 mL PBS containing 10 μg/mL RNase for 30 minutes at room temperature, and analyzed for DNA content by Cytomics FC 500 Flow Cytometer (Beckman Coulter, Fullerton, CA).

Apoptosis assay

Apoptotic MM cells were detected using the annexin V–biotin apoptosis detection kit (Oncogene Research Products, San Diego, CA). Untreated or EGCG-treated myeloma cells (1×10^6 cells/mL) were mixed with annexin V–biotin and media-binding reagent and incubated in the dark for 15 minutes at room temperature. Cells were then centrifuged and medium was replaced with 1 × binding buffer (Oncogene Research Products) containing fluorescein isothiocyanate (FITC)–streptavidin (Amersham Life Sciences, Arlington Heights, IL). A portion of cell suspension (50 μL) was placed onto a glass slide, covered with a coverslip, and viewed immediately using a fluorescence microscope equipped with a FITC (green) filter. Imaging was conducted as described in "siRNA and transfections." Two hundred cells, representing at least 5 distinct microscopic fields, were analyzed to assess the fraction of FITC-labeled cells for each sample.

Gene expression profile

Myeloma (INA6) cells, untreated or treated with 10 μM EGCG for 24 hours, were harvested and total RNA was isolated using an RNeasy kit (Qiagen, Valencia, CA) as described by the manufacturer. Total RNA (10-15 μg) was reverse-transcribed to get cDNA using the Superscript II reverse transcription kit (Invitrogen Life Technologies, Carlsbad, CA). cDNA was used in an in vitro transcription reaction to synthesize biotin-labeled cRNA using the Enzo RNA labeling kit (Enzo Diagnostics, Farmingdale, NY). Labeled cRNA was purified with the RNeasy mini-kit (Qiagen, Valencia, CA) and quantitated. Purified cRNA (15 μg) was hybridized to Human Genome U133 (HG-U133) GeneChip arrays (Affymetrix, Santa Clara, CA) according to the manufacturer's protocol. The HG-U133 set consists of 2 GeneChip arrays representing approximately 33 000 human genes. GeneChip arrays were scanned on a GeneArray scanner (Affymetrix).

Microarray data analysis

Normalization of arrays and calculation of expression values was performed using the DNA-chip analyzer (dChip) program.[26,27] Arrays were normalized based on relative signal produced for an invariant subset of genes. This model-based method was used for probe selection and computing expression values.[26,27] By pooling hybridization information across multiple arrays, it is possible to assess standard errors for the expression level indexes. This approach also allows automatic probe selection in the analysis stage to reduce errors due to cross-hybridization of probes and image contamination. We also used several high-level analysis functions in dChip for comparative analysis and hierarchic clustering.

Western blotting

Approximately 50 mg protein was suspended in Laemmli sample buffer (0.1 M Tris-HCl buffer, pH 6.8, 1% SDS, 0.05% β-mercaptoethanol, 10% glycerol, and 0.001% bromphenol blue), boiled for 2 minutes, and electrophoresed on 4% to 20% glycerol gradient SDS-polyacrylamide gel for 4 hours at 120 V. Gels were electroblotted onto Trans-Blot nitrocellulose membrane (Bio-Rad Laboratories, Hercules, CA) at 40 V for 3 hours in a Tris-glycine buffer system. Incubation with indicated antibodies was performed for 2 hours in PBS-Tween 20 (PBST) containing 1% BSA with constant rocking. Blots were washed with PBST and incubated in either anti–rabbit or anti–mouse horseradish peroxidase (HRP) conjugates for 2 hours in PBST containing 3% nonfat dry milk. After washing, specific

proteins were detected using an enhanced chemiluminescence, according to the instructions provided in the manual (Amersham Life Sciences).

Results

EGCG induces inhibition of myeloma cell growth

INA6, ARP, and OPM1 MM cells were cultured in the presence or absence of EGCG at various concentrations and for variable lengths of time and viable cell number was determined as described. EGCG induced both time- and dose-dependent decline in survival of myeloma cells; at 10 μM concentration it induced 85% and over 55% cell death in INA6 and ARP myeloma cells, respectively, at day 3 and more than 99% cell death in INA6 and ARP cell lines at day 5 and OPM1 cells at day 7 (Figure 1A-C). In all myeloma cell lines tested and primary myeloma cells derived from 3 different patients, exposure to 10 or 20 μM EGCG led to a significant inhibition of cell proliferation as assessed by ^{3}H-thymidine incorporation, within 72 hours treatment (Figure 1D-E). Importantly, the same concentrations of EGCG (10 or 20 μM) had no effect on survival of normal diploid fibroblasts and normal PBMCs from 4 healthy donors (Figure 1F-G). Normal PBMCs were treated with EGCG and cell proliferation was assessed by trypan blue exclusion or ^{3}H-thymidine incorporation or both. As seen in Figure 1G, EGCG at 10 or 20 μM had no effect on cell proliferation following 72 hours of treatment. To further confirm the lack of effect on normal cells, normal PBMCs were activated with anti-CD3 antibody and treated with EGCG. As indicated by ^{3}H-thymidine incorporation, exposure to 10 μM EGCG did not have inhibitory effect on proliferation of PBMCs. These data confirm that EGCG, at concentrations used, specifically inhibits the proliferation of myeloma cells while having no significant effect on normal cells.

EGCG induces apoptotic cell death

Myeloma cells (INA6 and ARP) were treated with EGCG (10 μM) and analyzed for apoptotic cell death. Both untreated or EGCG-treated myeloma cells were sequentially treated with annexin V–biotin and FITC-streptavidin and apoptotic cells were evaluated by a fluorescence microscope. Approximately 200, representing at least 5 distinct microscopic fields, were analyzed to assess the fraction of annexin V$^+$ cells for each sample. Following a 3-day exposure to EGCG, 92% ± 8% INA6 cells and 73% ± 6% of ARP cells were annexin V$^+$, whereas only 8% ± 2% and less than 2% of untreated INA6 and ARP cells, respectively, were annexin V$^+$ (Figure 2), indicating that EGCG induces apoptosis in myeloma cells.

EGCG mediates its activity via LR1

EGCG has been reported to confer its effects through its interaction with LR1 (67 kDa).[28] We therefore evaluated the protein levels of LR1 in myeloma cell lines and patient samples using Western blot analysis. As seen in Figure 3Ai and quantitation following normalization with α-tubulin levels (Figure 3Aii), a 10-fold or greater increase in the protein levels of LR1 in all myeloma cell lines and patient samples is observed.

Next, to confirm the role of LR1 in EGCG-mediated growth inhibition of MM cells, we transfected INA6 myeloma cells with Cy3-labeled nontargeting control siRNA or siRNA directed against LR1. Uptake of siRNA was confirmed by fluorescence microscopy (Figure 3B), and reduction of LR1 protein level was confirmed by Western blot analysis (Figure 3C). Transfected cells were treated on the next day with EGCG (10 μM) and cell viability was measured on alternate days for 7 days. As seen in Figure 3D, EGCG had no significant effect on the growth of INA6 cells transfected with LR1-specific siRNA, whereas more than 98% of cells transfected with control siRNAs died within 3 days following exposure to EGCG.

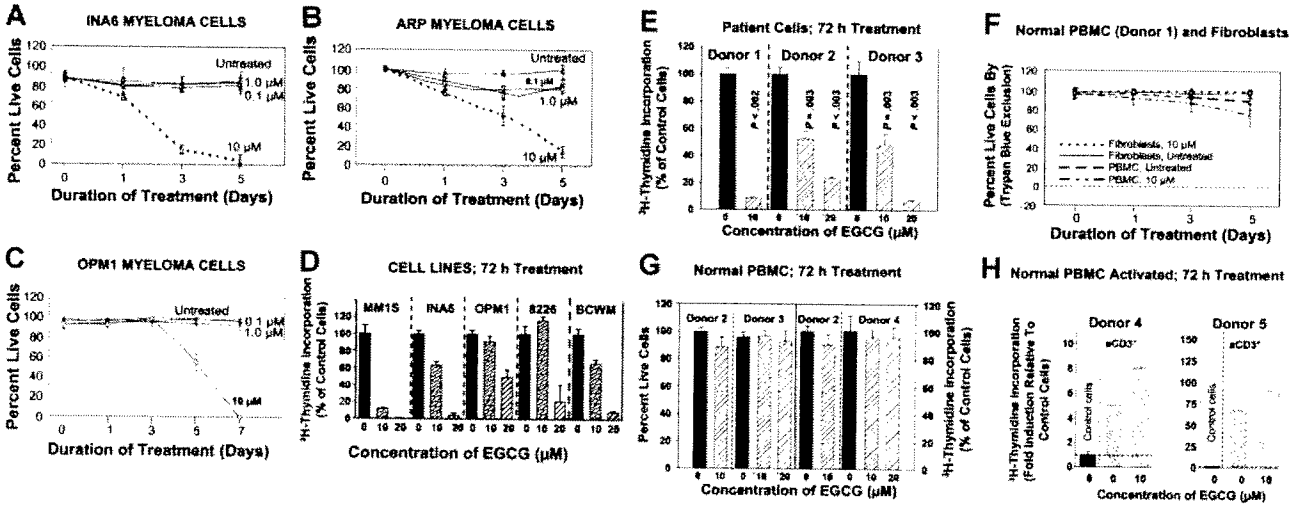

Figure 1. Effect of EGCG on cell survival. MM cells were cultured in the medium containing no EGCG or various concentrations of EGCG ranging from 0.1 to 10 μM. Cells were harvested at different time points as indicated and proliferative potential was assessed by trypan blue exclusion or ^{3}H-thymidine labeling. The growth curves show the mean of 3 independent experiments, with SEM. (A) IL-6–dependent INA6 myeloma cells. (B) ARP myeloma cells. (C) OPM1 myeloma cells. (D) Myeloma cell lines MM1S, INA6, OPM1, 8226, and Waldenstrom cells (BCWM) were treated with 10 and 20 μM EGCG for 72 hours and proliferative potential was assessed by ^{3}H-thymidine incorporation. (E) Three samples of CD138$^-$ purified myeloma cells derived from patient bone marrow were treated with 10 and 20 μM EGCG for 72 hours and cell proliferation was evaluated by ^{3}H-thymidine incorporation. (F) Effect of EGCG treatment in normal diploid fibroblasts and PBMCs from a healthy donor at days 1, 3, and 5. (G) Effect of EGCG on proliferation of PBMC from healthy donors is shown by trypan blue exclusion and ^{3}H-thymidine incorporation, following 72 h treatment with 10 and 20 μM drug. (H) PBMCs from healthy donors (donors 4 and 5) were activated with anti-CD3 antibody, treated with 10 μM EGCG for 72 hours, and cell proliferation was evaluated by ^{3}H-thymidine incorporation.

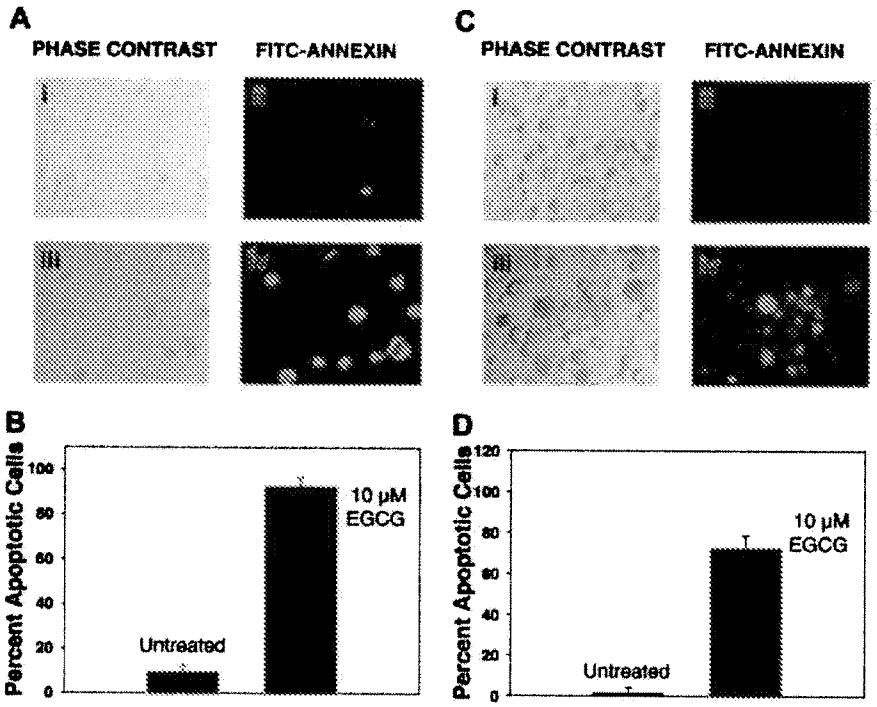

Figure 2. Apoptosis following EGCG treatment of myeloma cells. Myeloma cells were treated with 10 μM EGCG for 72 hours and analyzed for apoptosis using annexin V–biotin apoptosis detection kit. Cells were sequentially treated with annexin V–biotin and FITC-streptavidin. FITC-streptavidin–labeled apoptotic cells within the same microscopic field were viewed and photographed by phase contrast (PC) or by fluorescence emitted at 518 nm (FITC filter). Using the FITC filter, apoptotic cells appear bright green. (A) INA6 myeloma cells, untreated (i-ii) or treated with EGCG (iii-iv). (B) Bar graph shows percent apoptotic cells in control or EGCG-treated INA6 cells. (C) ARP myeloma cells, untreated (i-ii) or treated with EGCG (iii-iv). (D) Bar graph shows percent apoptotic cells in control or EGCG-treated ARP cells. (B, D) Error bars indicate SEM of percentage of apoptotic cells in 5 distinct microscopic fields.

EGCG induces apoptosis in myeloma cells in vivo

To evaluate in vivo activity of EGCG on MM cells, OPM1 MM cells were injected subcutaneously in CB17/ICr-SCID mice, and following appearance of palpable tumors, mice were given intraperitoneal injections of PBS alone or EGCG dissolved in PBS. As the tumors reached more than 2 cm in size, the mice were humanely killed, the tumors were excised, and the cell-cycle profile of MM cells was analyzed using PI staining and flow cytometry. Percentage of apoptotic cells in tumors derived from 3 control mice remained less than 1%, whereas the fraction of apoptotic cells in EGCG-treated mice ranged from 32% to 39%, indicating significant ($P < .004$) in vivo antimyeloma activity.

Consistent with these data, the survival of EGCG-treated mice was also prolonged relative to control mice (Figure 4B).

EGCG activates multiple proapoptotic pathways

To identify the molecular mechanisms of EGCG-induced apoptosis, we analyzed change in gene expression profile of INA6 cells following exposure to 10 μM EGCG for 24 hours, using HG-U133A GeneChip array (Affymetrix), as reported previously.[20,21,29,30] Reproducibility of expression change was confirmed by correlation coefficients (0.96-0.99) of independently conducted experiments.

Exposure of myeloma cells to EGCG led to up-regulation of major regulatory genes involved in apoptosis and cell cycle arrest

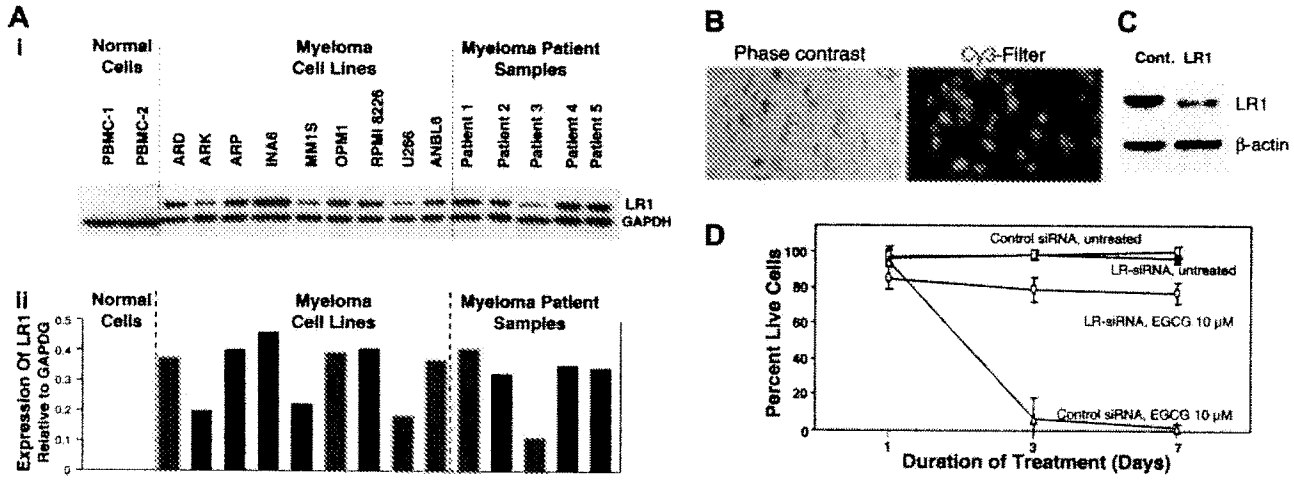

Figure 3. Role of LR1 in EGCG-induced myeloma cell death. (A) Elevated levels of LR1 (67 kDa) protein in myeloma cells. (Ai) Protein levels of LR1 were evaluated in 2 samples of normal PBMCs, 9 myeloma cell lines, and 5 myeloma patient samples, using a monoclonal antibody specific for LR; (ii) bar graph shows expression of LR1 protein, normalized to GAPDH levels, in normal and myeloma cells. (B-C) INA6 myeloma cells were cotransfected with Cy3-labeled nontargeting control (cont) and laminin receptor 1 (LR1) siRNAs. (B) Transfected cells were incubated for 72 hours and uptake of siRNA was monitored by a fluorescence microscope equipped with a Cy3 filter. (C) INA6 cells were transfected as described for panel B and LR1 protein level was determined by Western blot analysis. (D) EGCG induced myeloma cell death. INA6 myeloma cells were transfected with control siRNAs or siRNAs directed against LR1, and 24 hours later treated with 10 μM EGCG. Cell viability was determined on alternate days. Error bars indicate SEM of 3 independent experiments.

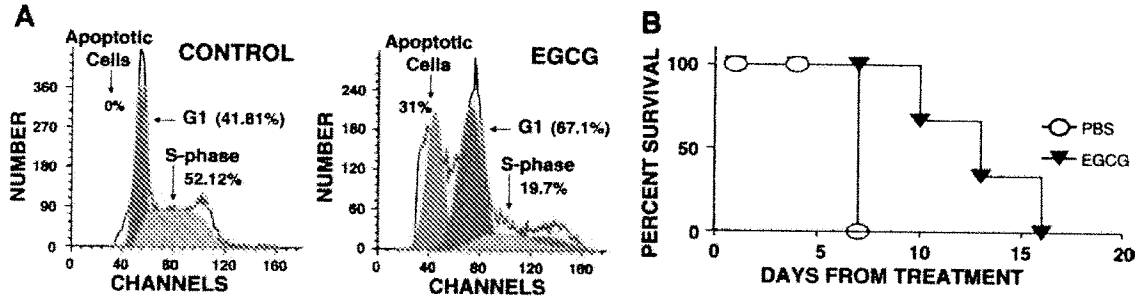

Figure 4. Effect of EGCG on proliferation of myeloma cells in vivo. CB-17 SCID mice were inoculated subcutaneously in the interscapular area with 5×10^6 OPM1 myeloma cells. Following appearance of tumors, the mice were treated intraperitoneally with PBS alone or EGCG 33 mg/kg/d. When mice were humanely killed, tumors were excised and analyzed for apoptosis by flow cytometry. (A) Cell-cycle profiles of tumor cells derived from control and EGCG-treated mice. (B) Survival curve of control and EGCG-treated mice.

as well as down-regulation of genes implicated in oncogenic transformation (Figure 5).

EGCG activated multiple pathways associated with growth arrest by inducing the expression of: (1) death-associated protein kinase 2 (DAPK2), a multifunctional protein kinase implicated in apoptotic pathways mediated by death receptors, p19/p53, and modulation of cytoskeleton; (2) initiators and mediators of death receptor–mediated apoptosis including Fas, Fas ligand, and caspase 4; (3) p63, a p53-like protein involved in induction of apoptosis; (4) caspase recruitment domain proteins (CARD10 and CARD14) associated with induction of apoptosis via activation of BCL10 and NF-κB; and (5) cyclin-dependent kinase inhibitors, p16 and p18 (Figure 5), which induce cell-cycle arrest by inhibiting phosphorylation of retinoblastoma (RB).

For selected genes, we have further confirmed the observed changes in gene expression profile at protein levels. Myeloma cells were treated with EGCG at 10 μM for 24 hours and the cell lysates were resolved on a gradient SDS-polyacrylamide gel, electroblotted, and probed with specific antibodies. Consistent with gene expression data, the exposure of MM cells to EGCG was associated with elevated protein levels of DAPK2, p18, and p63 (Figure 6A-D). Both the gene expression (not shown) and Western blot (Figure 6C-D) analyses indicated no change in level of p53 following exposure to EGCG. However, the Western blot analysis indicated a 6-fold increase in p73 protein (Figure 6C-D). Overall these data confirm the gene expression and protein changes and provide the molecular basis for observed growth arrest and apoptosis following exposure of myeloma cells to EGCG.

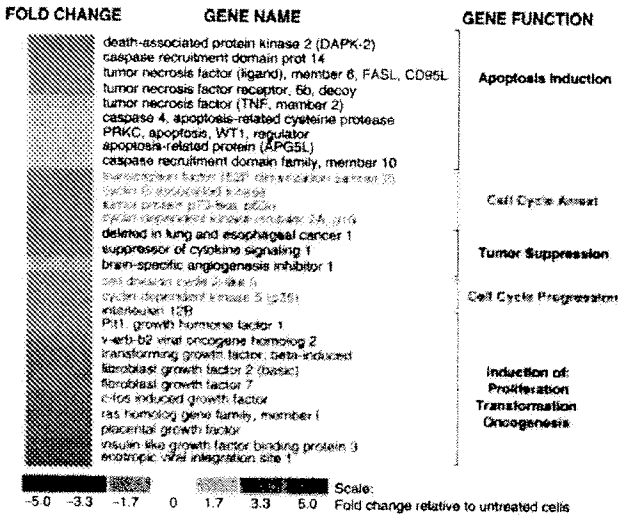

Figure 5. Effect of EGCG on gene expression in myeloma cells. Gene expression profile was analyzed in untreated or EGCG-treated (10 μM for 24 hours) MM cells using HG-U133A gene arrays (Affymetrix). Fold change in the expression in EGCG-treated cells relative to expression in untreated INA6 cells is shown by the intensity of red (induction) or blue (suppression) colors.

Discussion

Here, we demonstrate that EGCG, an antioxidant from green tea, induces growth arrest and apoptosis in MM cells while having no significant effect on normal PBMCs as well as fibroblasts. Anticancer effects of EGCG have been demonstrated in vitro in several malignancies including human lung, cervical, colon, and oral squamous carcinoma cells with effective IC_{50} values ranging from 22 to 200 μM.[14,18,31] However, this is the first report demonstrating its activity in hematologic malignancy and elucidating the molecular mechanisms of EGCG-induced apoptosis in cancer cells, specifically in MM. Exposure of

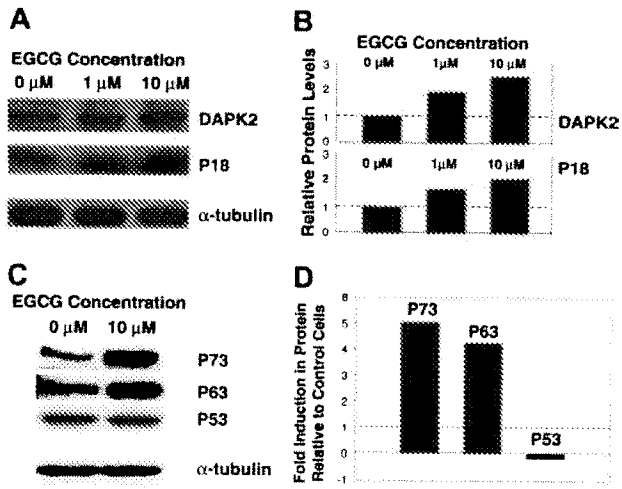

Figure 6. The effect of EGCG on protein expression in INA6 myeloma cells. Equal amounts of protein were fractionated on SDS-polyacrylamide gels and electroblotted onto nitrocellulose membranes. The membranes were sequentially treated with primary antibodies and HRP-conjugated secondary antibodies, and the proteins were detected using an enhanced chemiluminescence. The same blots were then stripped and incubated with a monoclonal antibody for α-tubulin. Signal intensity of each band was quantitated and the amount of each protein was normalized to that of α-tubulin. (A) Expression of DAPK2 and p18 proteins in INA6 cells, untreated or treated with 1 μM and 10 μM EGCG for 24 hours. (B) Bar graph shows relative expression of DAPK2 and p18 proteins, following normalization with corresponding α-tubulin levels. (C) Expression of p53 family of proteins (p53, p63, p73) in INA6 cells, untreated or treated with 10 μM EGCG for 24 hours. (D) Bar graph shows fold induction of p53 family members, following normalization with corresponding α-tubulin levels.

myeloma cell lines and primary patient cells to 10 to 20 μM EGCG led to apoptotic cell death within 5 to 7 days. Our data suggest higher susceptibility of MM cells to EGCG, which may provide a higher therapeutic index. Importantly EGCG at 10 to 20 μM had no significant effect on survival or proliferation of normal diploid fibroblasts and normal PBMCs.

To further confirm the lack of its effect on normal cells, we treated normal PBMCs activated with anti-CD3 antibody with EGCG at 10 μM (Figure 1H) and 20 μM (data not shown) and observed no effect on ^{3}H-thymidine incorporation. These data further confirm that EGCG specifically inhibits the proliferation of myeloma cells while having no effect on normal cells at a concentration that can be achieved in vivo, as demonstrated in a rat model in which plasma concentration of 96.0 μM was achieved without reported toxicity.[32]

We have also confirmed in vivo activity of EGCG in MM. Administration of EGCG at 33 mg/kg/d led to induction of apoptosis in MM cells and prolongation of survival in SCID mice bearing subcutaneous MM tumors. The survival of EGCG-treated mice was also significantly increased ($P < .05$), demonstrating an antimyeloma activity in vivo.

We also demonstrate that the antimyeloma effects of EGCG are mediated through a 67-kDa LR1, a cell-surface receptor implicated in the interaction of myeloma cells with basement membrane and subsequent infiltration/migration of these cells in surrounding tissue.[33] As reported here, LR1 knock-down cells are not susceptible to EGCG-induced myeloma cell death. The majority of myeloma cell lines and patient samples have elevated levels of LR1 protein. Gene expression profiling also showed up-regulated transcript levels of LR1 and its pseudogene in primary patient myeloma cells compared to normal plasma cells (data not shown). Extremely low expression of LR1 in normal cells and overexpression in myeloma cells provides the molecular explanation for specific activity of EGCG on MM cells with minimum effect on normal cells and may also provide the basis on which to expect a higher pharmacologic index for this agent in clinical practice.

The gene expression profile following EGCG treatment showed the most prominent induction of death-associated protein kinase 2 (DAPK2). DAPK2, a member of calcium/calmodulin-dependent serine/threonine kinases,[34] is implicated in multiple apoptotic pathways. Apoptosis initiated by TNF-α, activated Fas, and IFN-γ is mediated by DAPK,[35] which functions as a key regulatory step between the formation of death-inducing signaling complex (DISC) and activation of caspases.[35,36] DAPK can also induce apoptosis by p19ARF-p53 pathway[37,38] as well as by phosphorylation of myosin light chain, which leads to abnormal cytokinesis.[36]

EGCG treatment was also associated with elevated transcript and protein levels of p73 and p63, the members of the p53 family with ability to induce apoptosis in a p53-like manner.[39,40] Because p53 is frequently mutated in cancers, the induction of p53-like proteins (p73 and p63) by EGCG provides an important alternate mechanism of cell growth arrest in the absence of p53. These proteins are not only implicated in the induction of genes involved in apoptosis but also regulate genes involved in cell-cycle arrest and DNA repair.

EGCG also induced the expression of tumor necrosis factor ligand (member 6; FASL) and tumor necrosis factor receptor (member 6b; FAS), implicated in the death receptor–dependent apoptosis. The interaction between the ligand and its death receptor leads to the recruitment of DISC that subsequently initiates a cascade of events leading to activation of initiator and effector caspases. An in vitro evaluation in liver cancer has confirmed the increased protein levels of FASL following EGCG treatment.[41] There is also evidence that EGCG may directly bind and activate FAS leading to induction of apoptosis.[42]

Both gene expression and protein data also indicate that EGCG treatment is associated with the induction of cyclin-dependent kinase (CDK) inhibitors p16 and p18. Inhibitors of CDKs can induce cell-cycle arrest by preventing RB phosphorylation and E2F1 release.

In conclusion, these studies demonstrate that EGCG is a potent suppressor of MM cell growth with specificity provided by its interaction with LR1, a cell-surface receptor implicated in the interaction of myeloma cells with basement membrane. It leads to induction of multiple interrelated pathways implicated in growth arrest, providing a concerted activity leading to MM cell death both in vitro and in vivo. These data, therefore, indicate that a natural product with antioxidant properties from green tea has a specific activity against MM, making it an ideal compound for therapy and possible chemoprevention of this disease.

References

1. Brown MD. Green tea (*Camellia sinensis*) extract and its possible role in the prevention of cancer. Altern Med Rev. 1999;4:360-370.
2. Ahmad N, Feyes DK, Nieminen AL, Agarwal R, Mukhtar H. Green tea constituent epigallocatechin-3-gallate and induction of apoptosis and cell cycle arrest in human carcinoma cells. J Natl Cancer Inst. 1997;89:1881-1886.
3. Borska S, Gebarowska E, Wysocka T, Drag-Zalesinska M, Zabel M. Induction of apoptosis by EGCG in selected tumour cell lines in vitro. Folia Histochem Cytobiol. 2003;41:229-232.
4. Chen ZP, Schell JB, Ho CT, Chen KY. Green tea epigallocatechin gallate shows a pronounced growth inhibitory effect on cancerous cells but not on their normal counterparts. Cancer Lett. 1998; 129:173-179.
5. Lambert JD, Yang CS. Mechanisms of cancer prevention by tea constituents. J Nutr. 2003;133: 3262S-3267S.
6. Morse MA, Kresty LA, Steele VE, et al. Effects of the flavins on N-nitrosomethylbenzylamine-induced esophageal tumorigenesis. Nutr Cancer. 1997;29:7-12.
7. Otsuka T, Ogo T, Eto T, Asano Y, Suganuma M, Niho Y. Growth inhibition of leukemic cells by (-)-epigallocatechin gallate, the main constituent of green tea. Life Sci. 1998;63:1397-1403.
8. Stoner GD, Mukhtar H. Polyphenols as cancer chemopreventive agents. J Cell Biochem Suppl. 1995;22:169-180.
9. Yang CS, Wang ZY. Tea and cancer. J Natl Cancer Inst. 1993;85:1038-1049.
10. Chow HH, Cai Y, Hakim IA, et al. Pharmacokinetics and safety of green tea polyphenols after multiple-dose administration of epigallocatechin gallate and polyphenon E in healthy individuals. Clin Cancer Res. 2003;9:3312-3319.
11. Cao Y, Cao R. Angiogenesis inhibited by drinking tea. Nature. 1999;398:381.
12. Garbisa S, Sartor L, Biggin S, Salvato B, Benelli R, Albini A. Tumor gelatinases and invasion inhibited by the green tea flavanol epigallocatechin-3-gallate. Cancer. 2001;91:822-832.
13. Lin JK, Liang YC, Lin-Shiau SY. Cancer chemoprevention by tea polyphenols through mitotic signal transduction blockade. Biochem Pharmacol. 1999;58:911-915.
14. Yang GY, Liao J, Kim K, Yurkow EJ, Yang CS. Inhibition of growth and induction of apoptosis in human cancer cell lines by tea polyphenols. Carcinogenesis. 1998;19:611-616.
15. Gao CM, Takezaki T, Wu JZ, et al. Glutathione-S-transferases M1 (GSTM1) and GSTT1 genotype, smoking, consumption of alcohol and tea and risk of esophageal and stomach cancers: a case-control study of a high-incidence area in Jiangsu Province, China. Cancer Lett. 2002; 188:95-102.
16. Gao YT, McLaughlin JK, Blot WJ, Ji BT, Dai Q, Fraumeni JF Jr. Reduced risk of esophageal cancer associated with green tea consumption. J Natl Cancer Inst. 1994;86:855-858.
17. Li ZG, Shimada Y, Sato F, et al. Inhibitory effects of epigallocatechin-3-gallate on N-nitrosomethylbenzylamine-induced esophageal tumorigenesis in F344 rats. Int J Oncol. 2002;21:1275-1283.
18. Ahn WS, Huh SW, Bae SM, et al. A major constituent of green tea, EGCG, inhibits the growth of a human cervical cancer cell line, CaSki cells, through apoptosis, G(1) arrest, and regulation of gene expression. DNA Cell Biol. 2003;22:217-224.
19. Fang MZ, Wang Y, Ai N, et al. Tea polyphenol (-)-epigallocatechin-3-gallate inhibits DNA methyltransferase and reactivates methylation-silenced

genes in cancer cell lines. Cancer Res. 2003;63: 7563-7570.

20. Shammas MA, Koley H, Beer DG, Li C, Goyal RK, Munshi NC. Growth arrest, apoptosis, and telomere shortening of Barrett's-associated adenocarcinoma cells by a telomerase inhibitor. Gastroenterology. 2004;126:1337-1346.
21. Shammas MA, Reis RJ, Li C, et al. Telomerase inhibition and cell growth arrest after telomestatin treatment in multiple myeloma. Clin Cancer Res. 2004;10:770-776.
22. Shammas MA, Shmookler Reis RJ, Akiyama M, et al. Telomerase inhibition and cell growth arrest by G-quadruplex interactive agent in multiple myeloma. Mol Cancer Ther. 2003;2:825-833.
23. Shammas MA, Shmookler Reis RJ, Li C, et al. Telomerase inhibition and cell growth arrest after telomestatin treatment in multiple myeloma. Clin Cancer Res. 2004;10:770-776.
24. Elbashir SM, Harborth J, Lendeckel W, Yalcin A, Weber K, Tuschl T. Duplexes of 21-nucleotide RNAs mediate RNA interference in cultured mammalian cells. Nature. 2001;411:494-498.
25. Harborth J, Elbashir SM, Bechert K, Tuschl T, Weber K. Identification of essential genes in cultured mammalian cells using small interfering RNAs. J Cell Sci. 2001;114:4557-4565.
26. Li C, Hung Wong W. Model-based analysis of oligonucleotide arrays: model validation, design issues and standard error application. Genome Biol. 2001;2:research0032.1-0032.11.
27. Li C, Wong WH. Model-based analysis of oligonucleotide arrays: expression index computation and outlier detection. Proc Natl Acad Sci U S A. 2001;98:31-36.
28. Tachibana H, Koga K, Fujimura Y, Yamada K. A receptor for green tea polyphenol EGCG. Nat Struct Mol Biol. 2004;11:380-381.
29. Davies FE, Dring AM, Li C, et al. Insights into the multistep transformation of MGUS to myeloma using microarray expression analysis. Blood. 2003;102:4504-4511.
30. Munshi NC, Hideshima T, Carrasco D, et al. Identification of genes modulated in multiple myeloma using genetically identical twin samples. Blood. 2004;103:1799-1806.
31. Elattar TM, Virji AS. Effect of tea polyphenols on growth of oral squamous carcinoma cells in vitro. Anticancer Res. 2000;20:3459-3465.
32. Isbrucker RA, Bausch J, Edwards JA, Wolz E. Safety studies on epigallocatechin gallate (EGCG) preparations, part 1: genotoxicity. Food Chem Toxicol. 2006;44:626-635.
33. Vande Broek I, Vanderkerken K, De Greef C, et al. Laminin-1-induced migration of multiple myeloma cells involves the high-affinity 67 kD laminin receptor. Br J Cancer. 2001;85:1387-1395.
34. Kawai T, Nomura F, Hoshino K, et al. Death-associated protein kinase 2 is a new calcium/calmodulin-dependent protein kinase that signals apoptosis through its catalytic activity. Oncogene. 1999;18:3471-3480.
35. Cohen O, Inbal B, Kissil JL, et al. DAP-kinase participates in TNF-alpha- and Fas-induced apoptosis and its function requires the death domain. J Cell Biol. 1999;146:141-148.
36. Ng MH. Death associated protein kinase: from regulation of apoptosis to tumor suppressive functions and B cell malignancies. Apoptosis. 2002;7:261-270.
37. Inbal B, Cohen O, Polak-Charcon S, et al. DAP kinase links the control of apoptosis to metastasis. Nature. 1997;390:180-184.
38. Raveh T, Kimchi A. DAP kinase-a proapoptotic gene that functions as a tumor suppressor. Exp Cell Res. 2001;264:185-192.
39. Dietz S, Rother K, Bamberger C, Schmale H, Mossner J, Engeland K. Differential regulation of transcription and induction of programmed cell death by human p53-family members p63 and p73. FEBS Lett. 2002;525:93-99.
40. Ishida S, Yamashita T, Nakaya U, Tokino T. Adenovirus-mediated transfer of p53-related genes induces apoptosis of human cancer cells.[erratum appears in Jpn J Cancer Res. 2000;91:767]. Jpn J Cancer Res. 2000;91:174-180.
41. Kuo PL, Lin CC. Green tea constituent (-)-epigallocatechin-3-gallate inhibits Hep G2 cell proliferation and induces apoptosis through p53-dependent and Fas-mediated pathways. J Biomed Sci. 2003;10:219-227.
42. Hayakawa S, Saeki K, Sazuka M, et al. Apoptosis induction by epigallocatechin gallate involves its binding to Fas. Biochem Biophys Res Commun. 2001;285:1102-1106.

Biochemical and Biophysical Research Communications 371 (2008) 172–176

Exhibit E

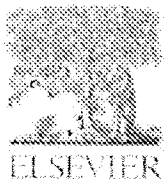

Contents lists available at ScienceDirect

Biochemical and Biophysical Research Communications

journal homepage: www.elsevier.com/locate/ybbrc

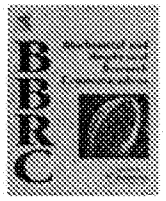

Involvement of 67-kDa laminin receptor-mediated myosin phosphatase activation in antiproliferative effect of epigallocatechin-3-*O*-gallate at a physiological concentration on Caco-2 colon cancer cells

Daisuke Umeda [a], Satomi Yano [a], Koji Yamada [a], Hirofumi Tachibana [a,b,*]

[a] *Laboratory of Food Chemistry, Division of Applied Biological Chemistry, Department of Bioscience and Biotechnology, Faculty of Agriculture, Kyushu University, Fukuoka 812-8581, Japan*

[b] *Laboratory of Functional Food Design, Department of Functional Metabolic Design, Bio-Architecture Center, Kyushu University, Fukuoka 812-8581, Japan*

ARTICLE INFO

Article history:
Received 8 April 2008
Available online 25 April 2008

Keywords:
Epigallocatechin-3-*O*-gallate
67-kDa laminin receptor
Cell cycle
Myosin regulatory light chain
Myosin phosphatase targeting subunit 1

ABSTRACT

Previously we reported that 67-kDa laminin receptor (67LR) mediates epigallocatechin-3-*O*-gallate (EGCG)-induced cell growth inhibition and reduction of myosin regulatory light chain (MRLC) phosphorylation at Thr-18/Ser-19, which is important for cytokinesis. Here, we found that human colon adenocarcinoma Caco-2 cells exhibited higher expression level of 67LR and EGCG at a physiologically achievable concentration (1 μM) significantly accumulated the cells in G_2/M phase without affecting expression of Wnt-signaling components. We also found that myosin phosphatase targeting subunit 1 (MYPT1) phosphorylation at Thr-696, which inhibits myosin phosphatase and promotes MRLC phosphorylation, was reduced in response to 1 μM EGCG. 67LR knockdown by RNA interference abolished the inhibitory effects of 1 μM EGCG on cell cycle progression and the phosphorylation of MRLC and MYPT1. These results suggest that through 67LR, EGCG at a physiological concentration can activate myosin phosphatase by reducing MYPT1 phosphorylation and that may be involved in EGCG-induced cell growth inhibition.

Green tea polyphenols have been shown to have cancer preventive activity in a variety of organ sites in animal models [1,2] and humans [3]. Among the green tea polyphenols, epigallocatechin-3-*O*-gallate (EGCG) is the most abundant and most active polyphenol in inhibiting experimental carcinogenesis and related reactions [2,4]. However, it is still not clear which EGCG-induced molecular events are responsible for the inhibition of carcinogenesis because the concentrations of EGCG shown to have an effect (20–100 μM) in most previous studies are much higher than the concentrations observed in the plasma or tissues of animals or in human plasma (usually lower than 1 μM) after tea ingestion [1]. Recently we have identified 67-kDa laminin receptor (67LR) as a cell surface EGCG receptor that mediates the anticancer action of physiologically achievable concentrations of EGCG (0.1–1 μM) [5]. Further others showed that RNA interference (RNAi)-mediated silencing of 67LR results in abrogation of EGCG-induced apoptosis in myeloma cells [6].

Myosin II, the conventional two-headed myosin first identified in muscle, is the primary motor protein responsible for cytokinesis [7]. It has been demonstrated that the contractile force of the contractile ring in dividing cells is generated by the association of myosin II with actin [7]. In higher eukaryotes, phosphorylation of the myosin regulatory light chain (MRLC) at Thr-18/Ser-19 increases the actin-activated Mg-ATPase activity of myosin II and the assembly of myosin II filaments, regulating the association between myosin II and actin [8]. Therefore, it is suggested that MRLC phosphorylation is crucial for cell division. Phosphorylation of MRLC is regulated by two classes of enzymes: MRLC kinases and myosin phosphatase [8]. Myosin phosphatase is composed with three subunits: a 37-kDa catalytic subunit, a 20-kDa subunit of unknown function, and a 110- to 130-kDa myosin phosphatase targeting subunit (MYPT1) [9]. The activity of myosin phosphatase is known to be regulated by phosphorylation of MYPT1 and two major sites, Thr-696 and Thr-853, have been extensively investigated and identified as an inhibitory site [9]. We previously reported that EGCG induced reduction of the phosphorylation of MRLC at Thr-18/Ser-19 through 67LR in HeLa cells [10], human basophilic KU812 cells [11] and mouse melanoma B16 cells [12], suggesting involvement of MRLC dephosphorylation in EGCG-induced cell growth inhibition. Further, we have reported that EGCG induced decrease in MYPT1 phosphorylation at Thr-696 through 67LR in HeLa cells and B16 cells, leading to activation of myosin phosphatase and reduction of MRLC phosphorylation [12].

* Corresponding author. Address: Laboratory of Food Chemistry, Division of Applied Biological Chemistry, Department of Bioscience and Biotechnology, Faculty of Agriculture, Kyushu University, 6-10-1 Hakozaki, Higashi-ku, Fukuoka 812-8581, Japan. Fax: +81 92 642 3008.

E-mail address: tatibana@agr.kyushu-u.ac.jp (H. Tachibana).

0006-291X/$ - see front matter © 2008 Elsevier Inc. All rights reserved.
doi:10.1016/j.bbrc.2008.04.041

Colorectal cancer is one of the most prevalent types of cancer in the Western world [13]. Epidemiological studies have suggested that the consumption of green tea may decrease colon cancer risk [14]. The Wnt-pathway appears to play an important role particularly in colon carcinogenesis [15]. The essential event in Wnt-signaling is the stabilization of β-catenin. The resulting accumulation of β-catenin increases the pool of nuclear β-catenin bound to transcription factor TCF/LEF in complexes that can activate certain genes, including oncogene c-Myc. As the main binding partner of β-catenin at cell–cell junctions, E-cadherin plays a pivotal role in β-catenin stabilization and function. E-cadherin commonly repressed in epithelial carcinogenesis and its binding with β-catenin suppressed Wnt-signaling [16]. Previous studies have reported that EGCG-treatment downregulated the β-catenin protein expression [17] or upregulated E-cadherin protein expression [18], suggesting that EGCG suppressed Wnt-signaling. However, it is still not known how a physiological concentration of EGCG induces cell growth inhibition in colorectal cancer cells. In this study, we found for the first time that a physiologically achievable concentration of EGCG inhibited cell cycle progression of human colon adenocarcinoma Caco-2 cells through 67LR without affecting components of Wnt-signaling. Further, we found that EGCG at a physiological concentration decreased the phosphorylation of MRLC at Thr-18/Ser-19 and MYPT1 at Thr-696 in Caco-2 cells through 67LR, suggesting that an activation of myosin phosphatase is involved in antiproliferative effect of EGCG at a physiological concentration.

Materials and methods

Materials and chemicals. EGCG, catalase, superoxide dismutase (SOD), and anti-β-actin antibody were purchased from Sigma Chemical Co. (St. Louis, MO). Anti-67LR (F-18) antibody, anti-MRLC (FL-172) antibody, horseradish peroxidase (HRP)-conjugated anti-mouse IgG and HRP-conjugated anti-goat IgG were obtained from Santa Cruz Biotechnology (Santa Cruz, CA). Anti-phospho-MRLC (Thr-18/Ser-19) antibody was obtained from Cell Signaling Technology, Inc. (Beverly, MA). Anti-MYPT1 antibody was purchased from BD Bioscience (San Jose, CA). Anti-phospho-MYPT1 (Thr-696) antibody was purchased from Upstate Biotechnology (Lake Placid, NY). HRP-conjugated anti-rabbit IgG antibody was obtained from ICN pharmaceuticals, Inc. (Costa Mesa, CA). Propidium iodide was obtained from Wako Pure Chemical Industries (Osaka, Japan).

Cell culture and cell proliferation assays. HeLa cells (a human cervical adenocarcinoma) were maintained in Dulbecco's modified Eagle's medium (DMEM) (COSMO BIO Co. Ltd., Tokyo, Japan) supplemented with 10% FBS (Biological Industries, Kibbutz Beit Kaemek, Israel) in a humidified atmosphere with 5% CO_2 at 37 °C. Caco-2 cells (a human colorectal adenocarcinoma) were maintained in DMEM supplemented with 10% FBS and 1% non-essential amino acid (NEAA) (Hyclone Inc., Logan, UT). To assess cell proliferation, cells were plated in 24-well plates at a density of 1×10^4 cells/well, and 24 h later they were treated with the indicated concentrations of EGCG for the indicated time periods in DMEM supplemented with 2% FBS, 1% NEAA (only for Caco-2 cells), 5 mg/mL BSA, 5 U/mL SOD and 200 U/mL catalase. Cell density was adhesive cell number per well.

Flow cytometric analysis. Cells were suspended in 70% ethanol and incubated at −20 °C for more than 4 h. The cells were washed with PBS and resuspended in PBS together with 10 μg/mL RNaseA. Incubation was continued at 37 °C for 20 min. The cellular DNA was then stained by applying propidium iodide (20 μg/mL) for 30 min at room temperature. The stained cells were analyzed by flow cytometry (FACS Calibur; Becton Dickinson, Sunnyvale, CA) for relative DNA content. ModFit LT software (Verity Software House, Inc., Topsham, ME) was used to assess cell cycle distribution.

Western blot analysis. Cells were lysed in cell lysis buffer containing 50 mM Tris–HCl (pH 7.5), 150 mM NaCl, 1% Triton X-100, 1 mM EDTA, 50 mM NaF, 30 mM $Na_4P_2O_7$, 1 mM phenylmethanesulfonyl fluoride, 10 μg/ml aprotinin, and 1 mM pervanadate. Proteins were subjected to sodium dodecyl sulfate–polyacrylamide gel electrophoresis (SDS–PAGE) and then transferred onto a nitrocellulose membrane. The membranes were blocked by BSA and incubated with primary antibodies, followed by incubation with HRP-conjugated secondary antibodies. Immunoreactive bands were visualized using the enhanced chemiluminescence Advance Western Blotting Detection kit (GE Healthcare, Little Chalfont, UK). Band intensities were quantified using NIH Image-J software.

RNA interference by shRNA. Target sequences for short hairpin RNAs for 67LR and nonspecific control are as follows: shRNA for 67LR, 5′-GGAGGAATTTCAGGGTGAA-3′; shRNA for nonspecific control, 5′-GCATATGTGCGTACCTAGCAT-3′. The annealed shRNA inserts were cloned into the the psiRNA-hH1neo shRNA expression vector (InvivoGen, San Diego, CA) according to the manufacturer's protocol. For stable transfection, FuGENE6 reagent (Roche, Basel, Switzerland) was mixed with DNA for 20 min in serum-free medium, the mixture was then added to Caco-2 cells in DMEM supplemented with 10% FBS and 1% NEAA. For stable transfection, the transfected cells were grown in medium containing G418.

Statistical analysis. All values are expressed as means ± SD compared with controls. Statistical analysis was performed by use of Student's t test. A level of $p < 0.05$ was considered significant.

Results

Caco-2 cells exhibited higher 67LR protein expression and sensitivity to EGCG than HeLa cells

We investigated the expression levels of 67LR in cervical adenocarcinoma HeLa cells and colorectal adenocarcinoma Caco-2 cells. Caco-2 cells exhibited higher 67LR protein expression than HeLa cells (Fig. 1A). We then examined antiproliferative effects of EGCG on HeLa cells and Caco-2 cells. EGCG inhibited the growth of Caco-2 cells in a dose-dependent manner (Fig. 1B) and the inhibitory effect was significantly observed even at 1 μM EGCG treatment (Fig. 1C). Compared with Caco-2 cells, HeLa cells were less sensitive to EGCG because its growth was inhibited at only 10 μM EGCG (Fig. 1B). These results suggest that the expression level of 67LR may be elevated in the cells that are sensitive to the effect of EGCG at a physiological concentration. To further determine the possible involvement of EGCG in the regulation of cell cycle, we subjected EGCG-treated cells to FACS analysis using propidium iodide staining to measure DNA content. EGCG dose-dependently decreased the G_0/G_1 and S fractions while increasing the G_2/M fraction in Caco-2 cells (Fig. 1D). The inhibition of cell cycle progression was significantly observed even at 1 μM EGCG. These results indicate that a physiologically achievable concentration of EGCG inhibited cell growth of Caco-2 cells by accumulating the cells in G_2/M phase.

Effect of EGCG on E-cadherin, β-catenin, and c-Myc protein expression in Caco-2 cells

We investigated the effect of EGCG on the protein expression of E-cadherin, β-catenin, and c-Myc, which are important Wnt-signaling components, in Caco-2 cells by Western blot analysis (Fig. 2). E-cadherin protein expression was not affected by EGCG at 1 or 5 μM, though it was slightly reduced by 10 μM EGCG treatment for 72 h. β-Catenin protein expression were slightly affected by EGCG at 1 or 5 μM but dose- and time-dependency were not observed. c-Myc protein expression was slightly reduced by 10 μM EGCG treatment for 72 h. Since these results did not correlate with EGCG-induced cell growth inhibition shown in Fig. 1, it is suggested that E-cadherin, β-catenin, and c-Myc are not involved in antiproliferative effect of EGCG at a physiological concentration on Caco-2 cells.

Effect of EGCG on the phosphorylation of MRLC and MYPT1 in Caco-2 cells and HeLa cells

To elucidate the intracellular mechanism of how EGCG accumulates Caco-2 cells in G_2/M phase, we examined the effect of EGCG on MRLC phosphorylation at Thr-18/Ser-19 by Western blot analysis. EGCG treatment for 24 h dose-dependently reduced the level of MRLC phosphorylation (Fig. 3A). To investigate how EGCG reduced MRLC phosphorylation, we tested the effect of EGCG on the phosphorylation of MYPT1 at Thr-696 and found that EGCG dose-dependently induced the dephosphorylation of MYPT1 at Thr-696 in Caco-2 cells (Fig. 3B). These results suggest that EGCG activated myosin phosphatase by reducing MYPT1 phosphorylation at Thr-696. Moreover, decrease in the phosphorylation of both MRLC and MYPT1 was observed even at 1 μM EGCG and correlated

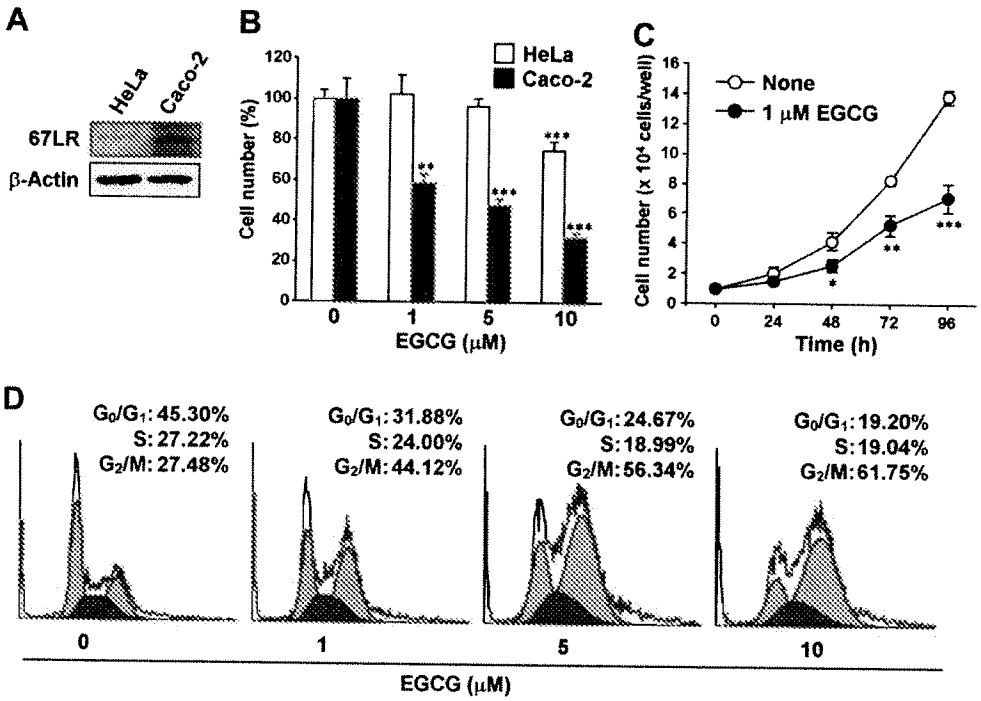

Fig. 1. Caco-2 cells exhibited higher 67LR protein expression and sensitivity to EGCG than HeLa cells. (A) Western blot analysis of 67LR in HeLa cells and Caco-2 cells. (B) The cells were treated with the indicated concentrations of EGCG for 96 h. (C) Caco-2 cells were treated with 1 μM EGCG for the indicated time periods. Data shown are means ± SD for three samples. Data containing asterisk marks are significantly different from the values in untreated control at $^{*}p < 0.05$, $^{**}p < 0.01$, or $^{***}p < 0.001$. (D) FACS analysis of the cell cycle. Cells were treated with the indicated concentrations of EGCG for 96 h. The cells were then evaluated for DNA content after propidium iodide staining.

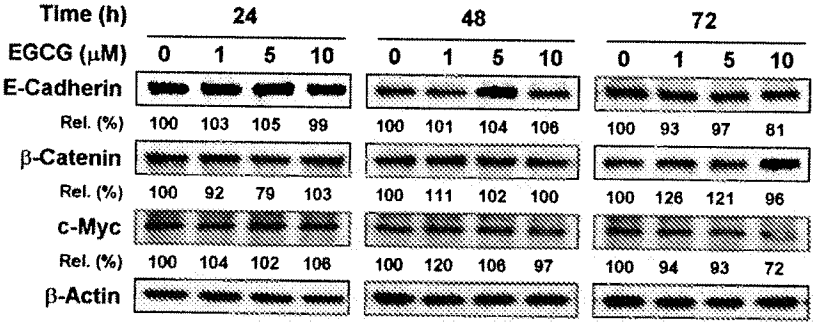

Fig. 2. Effect of EGCG on E-cadherin, β-catenin and c-Myc protein expression in Caco-2 cells. Cells were treated with the indicated concentrations of EGCG for the indicated time periods. Total cellular protein was subjected to Western blot analysis using anti-E-cadherin, anti-β-catenin and anti-c-Myc antibodies. Band intensity of each protein was normalized for β-actin and expressed as a percentage compared with the value of untreated control.

well with EGCG-induced cell growth inhibition shown in Fig. 1. The suppressive effects of EGCG at 1 μM on the phosphorylation of both MRLC and MYPT1 were still observed at 96 h after EGCG treatment in Caco-2 cells (Fig. 3C). In HeLa cells whose growth was not inhibited by 1 μM EGCG as shown in Fig. 1B , 1 μM EGCG did not affect the phosphorylation of either MRLC or MYPT1 (Fig. 3D). These results suggest that a physiologically achievable concentration of EGCG inhibited cell growth by reducing the phosphorylation of both MRLC and MYPT1 in Caco-2 cells.

Effect of 67LR knockdown on EGCG-induced cell growth inhibition and reduction of the phosphorylation of MRLC and MYPT1 in Caco-2 cells

To investigate whether the inhibitory effect of EGCG on cell cycle progression is mediated by 67LR, we knockdown the expression of 67LR in Caco-2 cells using RNAi-mediated gene silencing. We stably transfected Caco-2 cells with the short hairpin RNA (shRNA) expression vector for 67LR and confirmed the knockdown of 67LR protein expression in the cells (Fig. 4A). 67LR knockdown significantly attenuated 1 μM EGCG-induced inhibition of cell growth (Fig. 4B) and accumulation of the cells in G_2/M phase (Fig. 4C). Furthermore, 1 μM EGCG-induced reduction of the phosphorylation of both MRLC (The-18/Ser-19) and MYPT1 (Thr-696) was also attenuated in 67LR-shRNA expressing cells, suggesting that EGCG activated myosin phosphatase through 67LR (Fig. 4D). These results suggest that 67LR mediates the suppressive effect of EGCG at a physiological concentration on cell cycle progression and the phosphorylation of MRLC and MYPT1.

Discussion

Many mechanisms for anticarcinogenic activities of green tea polyphenol EGCG have been proposed based mainly on studies in cell lines [2,4]. The activities observed with EGCG in cell line studies, however, may not be relevant to the situation *in vivo* because EGCG concentrations used *in vitro* are usually much higher than the achievable levels *in vivo* [1,2]. Therefore, it is important to investigate the activities observed at physiologically achievable

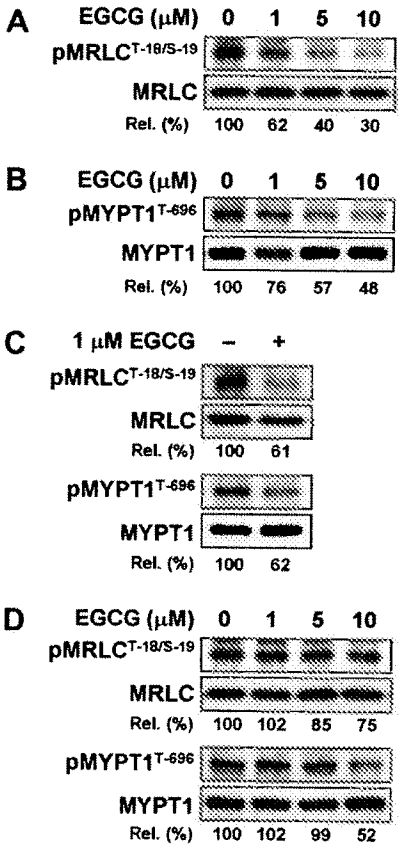

Fig. 3. Effect of EGCG on the phosphorylation of MRLC and MYPT1 in Caco-2 cells and HeLa cells. (A–C) Caco-2 cells were treated with the indicated concentrations of EGCG for 24 h (A and B) or treated with 1 μM EGCG for 96 h (C). (D) HeLa cells were treated with the indicated concentrations of EGCG for 24 h. Total cellular protein was subjected to Western blot analysis using anti-phospho-MRLC (Thr-18/Ser-19) and anti-phospho-MYPT1 (Thr-696) antibodies. Relative band intensity (pMRLC/MRLC or pMYPT1/MYPT1) was expressed as a percentage compared with the value of untreated control.

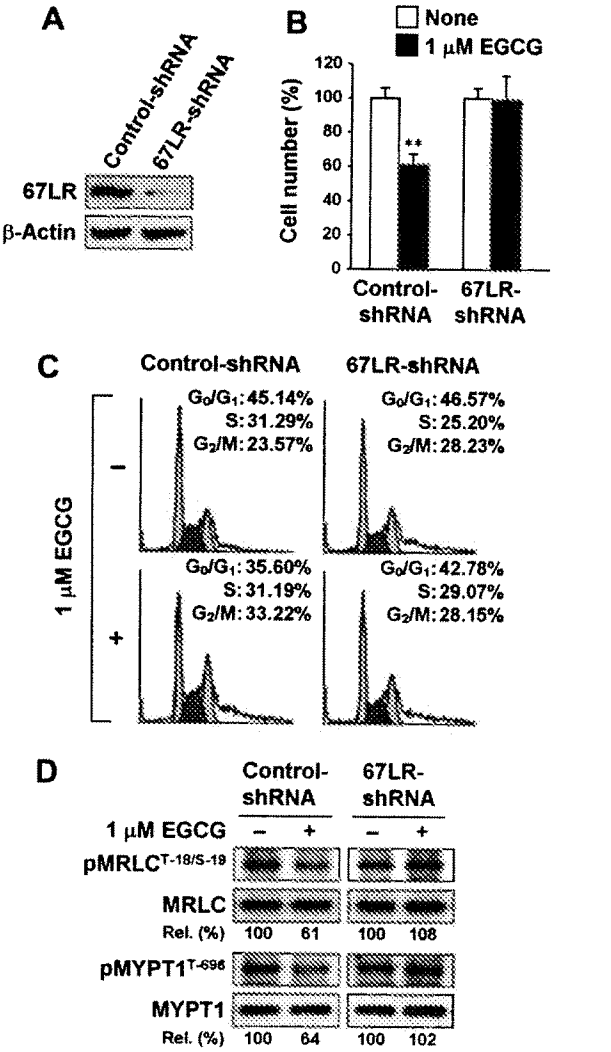

Fig. 4. Effect of 67LR knockdown on EGCG-induced cell growth inhibition and reduction of the phosphorylation of MRLC and MYPT1 in Caco-2 cells. (A) The cells stably transfected with the control-shRNA or the 67LR-shRNA expression vector were lysed and total cellular protein was subjected to Western blot analysis using anti-67LR antibody (F-18). (B) Cells were treated with 1 μM EGCG for 96 h. The results are shown as relative cell number to untreated control and the data presented are means ± SD for three samples. Data containing asterisk marks are significantly different from the values in control at $^{**}p < 0.01$. (C) FACS analysis of the cell cycle. Cells were treated as described in (B) and then evaluated for DNA content after propidium iodide staining. (D) Cells were treated with 1 μM EGCG for 24 h. Total cellular protein was subjected to Western blot analysis using anti-phospho-MRLC (Thr-18/Ser-19) and anti-phospho-MYPT1 (Thr-696) antibodies. Relative band intensity (pMRLC/MRLC or pMYPT1/MYPT1) was expressed as a percentage compared with the value of untreated control.

concentrations of EGCG. In the present study, we found that EGCG at a physiologically achievable concentration (1 μM) significantly inhibited cell growth of Caco-2 cells and accumulated the cells in G_2/M phase through 67LR. We also found that 1 μM EGCG reduced MYPT1 phosphorylation at Thr-696 through 67LR, leading to activation of myosin phosphatase and reduction of MRLC phosphorylation at Thr-18/Ser-19.

Several studies have reported that EGCG suppressed Wnt-signaling by affecting the protein levels of E-cadherin [18] and β-catenin [17], resulting in reduction of c-Myc and cyclin D1 [18]. On the other hand, many studies have reported that EGCG induces cell cycle arrest at G_0/G_1 phase in various cancer cells, including lung, colon, pancreas, skin, and prostate [1,3,5,19]. Since c-Myc and cyclinD1 are important cell cycle regulators particularly in the progression from G_1 to S phase [20], it may be proposed that suppression of Wnt-signaling by EGCG is the mechanism for EGCG-induced cell cycle arrest at G_0/G_1 phase. However, the concentrations of EGCG used in these previous studies are also much higher than those observed in the blood or tissues. In our experiment, a physiologically achievable concentration of EGCG accumulated Caco-2 cells in the G_2/M phase but not G_0/G_1 phase and did not affect the protein levels of E-cadherin, β-catenin and c-Myc. These results suggest that cell growth inhibition induced by a physiological concentration of EGCG in Caco-2 cells is dependent on other mechanisms than suppression of Wnt-signaling.

MRLC phosphorylation in cytokinesis can be regulated by myosin phosphatase and there are several pieces of evidence indicating that myosin phosphatase is involved in cytokinesis. MYPT1 is phosphorylated at the inhibitory sites at the cleavage furrow [21,22] and the MYPT1 phosphorylation is predicted to result in an increase in MRLC phosphorylation at the division site and might provide a signal for cytokinesis. MYPT mutations show effects on cytokinesis. In *Caenorhabditis elegans*, MYPT mutations cause defects in cytokinesis [23]. Mouse embryos lacking MYPT1 have recently been reported to die within 7.5 days post coitus, suggesting that mouse myosin phosphatase may be crucial for cytokinesis *in vivo* [24]. In our experiments, EGCG at a physiological concentration induced reduction of not only MRLC phosphorylation but MYPT1 phosphorylation at Thr-696 through 67LR, suggesting that EGCG activated myosin phosphatase and might prevent cytokinesis. It has also been reported that MYPT1 binds

to many other proteins in addition to phosphorylated MRLC and myosin phosphatase has several additional substrates [25]. Therefore, it is possible that dephosphorylation of not only MRLC but the other substrates by myosin phosphatase is critical for EGCG-induced cell growth inhibition through 67LR.

It is currently still unclear how EGCG exactly reduces MYPT1 phosphorylation at Thr-696 through 67LR. Most recently, we have identified eukaryotic translation elongation factor 1A (eEF1A) as a component responsible for the antiproliferative activity of EGCG [12]. Intriguingly, it has been reported that eEF1A binds to MYPT1 [26] and is localized in the cleavage furrow during cytokinesis [27], suggesting its involvement in cell division process. Although we have reported that eEF1A was involved in the signaling pathway mediated after binding of EGCG to 67LR, further studies are needed to define the role of eEF1A in decrease of MYPT1 phosphorylation at Thr-696. Future investigation on this matter and the *in vivo* role of 67LR, eEF1A and MYPT1 in EGCG-induced cell growth inhibition may provide new therapeutic approaches for the treatment of cancer.

Acknowledgment

This work was supported in part by Grants-in-Aid for Scientific Research (A) (to H.T.).

References

[1] C.S. Yang, P. Maliakal, X. Meng, Inhibition of carcinogenesis by tea, Annu. Rev. Pharmacol. Toxicol. 42 (2002) 25–54.
[2] C.S. Yang, S. Sang, J.D. Lambert, Z. Hou, J. Ju, G. Lu, Possible mechanisms of the cancer-preventive activities of green tea, Mol. Nutr. Food Res. 50 (2006) 170–175.
[3] S. Bettuzzi, M. Brausi, F. Rizzi, G. Castagnetti, G. Peracchia, A. Corti, Chemoprevention of human prostate cancer by oral administration of green tea catechins in volunteers with high-grade prostate intraepithelial neoplasia: a preliminary report from a one-year proof-of-principle study, Cancer Res. 66 (2006) 1234–1240.
[4] N. Khan, F. Afaq, M. Saleem, N. Ahmad, H. Mukhtar, Targeting multiple signaling pathways by green tea polyphenol (−)-epigallocatechin-3-gallate , Cancer Res. 66 (2006) 2500–2505.
[5] H. Tachibana, K. Koga, Y. Fujimura, K. Yamada, A receptor for green tea polyphenol EGCG, Nat. Struct. Mol. Biol. 11 (2004) 380–381.
[6] M.A. Shammas, P. Neri, H. Koley, R.B. Batchu, R.C. Bertheau, V. Munshi, R. Prabhala, M. Fulciniti, Y.T. Tai, S.P. Treon, R.K. Goyal, K.C. Anderson, N.C. Munshi, Specific killing of multiple myeloma cells by (−)-epigallocatechin-3-gallate extracted from green tea: biologic activity and therapeutic implications, Blood 108 (2006) 2804–2810.
[7] F. Matsumura, Regulation of myosin II during cytokinesis in higher eukaryotes, Trends Cell Biol. 15 (2005) 371–377.
[8] A.P. Somlyo, A.V. Somlyo, Ca^{2+} sensitivity of smooth muscle and nonmuscle myosin II: modulated by G proteins, kinases, and myosin phosphatase, Physiol. Rev. 83 (2003) 1325–1358.
[9] D.J. Hartshorne, M. Ito, F. Erdödi, Role of protein phosphatase type 1 in contractile functions: myosin phosphatase, J. Biol. Chem. 279 (2004) 37211–37214.
[10] D. Umeda, H. Tachibana, K. Yamada, Epigallocatechin-3-*O*-gallate disrupts stress fibers and the contractile ring by reducing myosin regulatory light chain phosphorylation mediated through the target molecule 67 kDa laminin receptor, Biochem. Biophys. Res. Commun. 333 (2005) 628–635.
[11] Y. Fujimura, D. Umeda, Y. Kiyohara, Y. Sunada, K. Yamada, H. Tachibana, The involvement of the 67 kDa laminin receptor-mediated modulation of cytoskeleton in the degranulation inhibition induced by epigallocatechin-3-*O*-gallate, Biochem. Biophys. Res. Commun. 348 (2006) 524–531.
[12] D. Umeda, S. Yano, K. Yamada, H. Tachibana, Green tea polyphenol epigallocatechin-3-gallate (EGCG) signaling pathway through 67-kDa laminin receptor, J. Biol. Chem. 283 (2008) 3050–3058.
[13] E.E. Calle, C. Rodriguez, K. Walker-Thurmond, M.J. Thun, Overweight, obesity, and mortality from cancer in a prospectively studied cohort of U.S. adults, N. Engl. J. Med. 348 (2003) 1625–1638.
[14] J.M. Yuan, Y.T. Gao, C.S. Yang, M.C. Yu, Urinary biomarkers of tea polyphenols and risk of colorectal cancer in the Shanghai Cohort Study, Int. J. Cancer 120 (2007) 1344–1350.
[15] F. Radtke, H. Clevers, Self-renewal and cancer of the gut: two sides of a coin, Science 307 (2005) 1904–1909.
[16] S. Orsulic, O. Huber, H. Aberle, S. Arnold, R. Kemler, E-cadherin binding prevents beta-catenin nuclear localization and beta-catenin/LEF-1-mediated transactivation, J. Cell Sci. 112 (1999) 1237–1245.
[17] W.M. Dashwood, O. Carter, M. Al-Fageeh, Q. Li, R.H. Dashwood, Lysosomal trafficking of beta-catenin induced by the tea polyphenol epigallocatechin-3-gallate, Mutat. Res. 591 (2005) 161–172.
[18] J. Ju, J. Hong, J.N. Zhou, Z. Pan, M. Bose, J. Liao, G.Y. Yang, Y.Y. Liu, Z. Hou, Y. Lin, J. Ma, W.J. Shih, A.M. Carothers, C.S. Yang, Inhibition of intestinal tumorigenesis in $Apc^{min/+}$ mice by (−)-epigallocatechin-3-gallate, the major catechin in green tea, Cancer Res. 65 (2005) 10623–10631.
[19] M. Shimizu, A. Deguchi, J.T. Lim, H. Moriwaki, L. Kopelovich, I.B. Weinstein, (−)-Epigallocatechin gallate and polyphenon E inhibit growth and activation of the epidermal growth factor receptor and human epidermal growth factor receptor-2 signaling pathways in human colon cancer cells, Clin. Cancer Res. 11 (2005) 2735–2746.
[20] S. Pelengaris, M. Khan, G. Evan, C-Myc: more than just a matter of life and death, Nat. Rev. Cancer 2 (2002) 764–776.
[21] Y. Kawano, Y. Fukata, N. Oshiro, M. Amano, T. Nakamura, M. Ito, F. Matsumura, M. Inagaki, K. Kaibuchi, Phosphorylation of myosin binding subunit (MBS) of myosin phosphatase by Rho-kinase *in vivo*, J. Cell Biol. 147 (1999) 1023–1037.
[22] T. Yokoyama, H. Goto, I. Izawa, H. Mizutani, M. Inagaki, Aurora-B and Rho-kinase/ROCK, the two cleavage furrow kinases, independently regulate the progression of cytokinesis: possible existence of a novel cleavage furrow kinase phosphorylates ezrin/radixin/moesin (ERM), Genes Cells 10 (2005) 127–137.
[23] A.J. Piekny, P.E. Mains, Rho-binding kinase (LET-502) and myosin phosphatase (MEL-11) regulate cytokinesis in the early *Caenorhabditis elegans* embryo, J. Cell Sci. 115 (2002) 2271–2282.
[24] R. Okamoto, M. Ito, N. Suzuki, M. Kongo, N. Moriki, H. Saito, H. Tsumura, K. Imanaka-Yoshida, K. Kimura, A. Mizoguchi, D.J. Hartshorne, T. Nakano, The targeted disruption of the MYPT1 gene results in embryonic lethality, Transgenic Res. 14 (2005) 337–340.
[25] F. Matsumura, D.J. Hartshorne, Myosin phosphatase target subunit: many roles in cell function, Biochem. Biophys. Res. Commun. 369 (2008) 149–156.
[26] T. Izawa, Y. Fukata, T. Kimura, A. Iwamatsu, K. Dohi, K. Kaibuchi, Elongation factor-1 alpha is a novel substrate of rho-associated kinase, Biochem. Biophys. Res. Commun. 278 (2000) 72–78.
[27] O. Numata, Y. Kurasawa, K. Gonda, Y. Watanabe, Tetrahymena elongation factor-1 alpha is localized with calmodulin in the division furrow, J. Biochem. 127 (2000) 51–56.